



Environmental and health costs of Europe's shift from gas to coal amidst the energy crisis

Mario Liebensteiner ^{id a,b,*}, Alex Mburu Kimani ^{id a}

^a Friedrich-Alexander-Universität (FAU) Erlangen-Nürnberg, Institute of Economic Research, Lange Gasse 20, 90403, Nuremberg, Germany

^b Energie Campus Nürnberg (EnCN), Germany

ARTICLE INFO

Keywords:

Air pollution
CO₂ emissions
Energy crisis
Gas price shock
Gas-to-coal switch
Health effects

ABSTRACT

The gas price explosion during the 2021/22 European energy crisis prompted a shift from gas to coal-fired electricity production. Empirical evidence on the environmental and health consequences of such a fuel-price shock – as opposed to policy reforms – is scarce. We fill this gap by quantifying how gas price surges reorder coal-gas marginal costs and, in turn, affect emissions and health outcomes. Using daily data (2015–2023) for six EU countries with substantial gas-to-coal switching potential, we estimate a control-function model (2SRI) to obtain causal effects of days on which gas is more expensive than coal. During the 510 days of the 2021/22 gas price surge when coal was cheaper, coal-fired generation rose by 23 %, driving a 10 % increase in CO₂, 19 % in PM_{2.5}, 10 % in NO_x, and 24 % in SO₂. We also report illustrative health implications by mapping our primary results to standard literature-based damage factors; the resulting figures are not observed health outcomes but order-of-magnitude indicators. All figures are computed relative to a model-based counterfactual in which gas remained the cheaper option and represent short-term effects that disregard longer-term structural adjustments. The results highlight the substantial welfare costs of fuel price shock-induced switching and inform the design of policies that internalize these externalities. We also discuss how these results should be interpreted within the EU ETS and the resulting “waterbed effect”.

1. Introduction

The escalation of tensions between Russia and Ukraine in mid-2021 caused significant upheaval in energy markets (Weitzel et al., 2024). In late 2021, Russia started disrupting gas deliveries to Europe, which struck at a crucial time, as Russia had long been the primary supplier of natural gas to Europe (Kotek et al., 2023).¹ In February 2022, the Russian invasion of Ukraine ultimately led to a skyrocketing gas price, as Fig. 1(a) shows. Although prices of other commodities also rose, the sharp increase in gas prices significantly heightened the relative marginal costs of gas-fired power plants compared to other electricity sources.

The core contribution of this study is to identify the causal effect of the 2021/22 gas price surge on electricity dispatch. When gas became more expensive than coal, systems relying on both technologies shifted from gas to coal. We quantify this market-driven

* Corresponding author.

E-mail addresses: mario.liebensteiner@fau.de (M. Liebensteiner), alex.kimani@fau.de (A.M. Kimani).

¹ However, other factors also contributed to high electricity and gas prices in Europe, such as the economic recovery after the COVID pandemic, a drought that reduced nuclear electricity supply in France due to cooling issues, lower-than-usual gas storage levels in Europe due to a cold winter and Gazprom's strategic behavior (Milov, 2022), and a higher demand for liquefied natural gas (LNG) in Asia and Latin America (EMBER, 2024; Ruhnau et al., 2023).

switching using a two-stage residual inclusion design on daily data from 2015 to 2023, including rich controls and fixed effects. Since direct emissions data for the power sector are not available, we convert electricity generation data into CO₂ and local pollutant emissions using standard engineering emission and efficiency factors, and we estimate the emissions impacts of the fuel switch. In addition, we report health and damage figures by mapping electricity generation data to literature-based damage factors. As these figures are not derived from observed health data, they should be interpreted as order-of-magnitude implications of the dispatch effect rather than as additional causal evidence.

Our empirical panel comprises six EU countries with significant gas-to-coal switching potential: Czechia, Germany, Ireland, Italy, the Netherlands, and Poland (further details on the country selection are provided in [Section 3.1](#)). These countries have both coal (lignite and/or hard coal) and gas generation capacities, enabling them to shift dispatch in response to relative-cost shocks triggered by the gas price surge during the 2021/22 energy crisis.

Historically, the price of gas was higher than the price of hard coal and lignite. Consequently, coal-fired power plants traditionally received priority dispatch over gas-fired power plants in the electricity supply function. From an environmental standpoint, this resulted in high CO₂ emissions and air pollution, as lignite and hard coal have significantly higher emission factors compared to gas. In late 2017, following reforms of the EU Emissions Trading System (ETS), the price of CO₂ allowances began to climb. This resulted in higher costs for coal-fired electricity production compared to gas-fired electricity. Consequently, there was a coal-to-gas switch in the merit order, leading to a significant reduction in electricity-related CO₂ emissions. However, despite high carbon prices, the explosion of gas prices during the energy crisis eventually caused a reverse switch from gas to coal, thereby raising emissions once again.

The results of this study are that coal-fired electricity production increased significantly, by 53 TWh (95 % CI: 43–63 TWh) or 23 %, during the 510 switching days when gas-fired electricity was more expensive than coal. Moreover, using our observed fuel-specific generation data applied to standard emission and efficiency factors, we find that the intensified coal combustion led to higher CO₂ and local air pollution. We estimate increases of 36 million metric tons (Mt) of CO₂ (95 % CI: 28–45 Mt; or 10 %), 187 t PM_{2.5} (95 % CI: 152–222 t; 19 %), 8,645 t NO_x (95 % CI: 6,573–10,715 t; 10 %), and 16,304 t SO₂ (95 % CI: 10,947–21,658 t; 24 %) across the studied countries. The largest effects are found for Germany, but even in Ireland's smaller system the effect is non-negligible. Finally, we report illustrative health implications from literature-based damage factors: indicative premature deaths and serious illnesses rose by about 17 %.

This study carries significant implications. Foremost, it is essential to quantify the environmental impact of a fuel price shock induced by the energy crisis. The study measures a notable increase in coal-based emissions resulting from the surge in gas prices. One concern with quantifying the increase in power-sector CO₂ emissions resulting from a gas price shock is the so-called "waterbed effect" ([Rosendahl, 2019](#)). The EU Emissions Trading System (EU ETS) puts a cap on CO₂-equivalent emissions from electricity production, energy-intensive industries, and aviation. Consequently, for a fixed supply of emission certificates, any CO₂ increase in one sector must be offset elsewhere ([Herweg and Schmidt, 2022](#)).

Nevertheless, an increase in power-sector emissions could have significant implications for the national carbon budgets of affected countries, potentially jeopardizing their national climate goals, especially the sector-specific goals set for the energy sector. Moreover, intensified coal-fired electricity production exacerbates significant adverse health effects through the emission of higher levels of local air pollutants ([Deschenes et al., 2017](#); [Holland et al., 2020](#); [Jarvis et al., 2022](#)), which are not regulated by the EU ETS. This may have led to increased health problems and even premature deaths among citizens of the affected countries ([Henneman et al., 2023](#); [Ritchie, 2020](#)).

The analysis also aids our understanding of the importance of natural gas in electricity supply. While there is a debate about whether gas can and should serve as a bridging technology along the path to decarbonization ([Gillingham and Stock, 2018](#)), the results demonstrate that a shock to gas supply has significant environmental consequences. Specifically, our findings suggest that gas-fired electricity production cannot be readily replaced by less-emissive supply technologies, such as renewable energies or nuclear power. Instead, dispatchable coal plants typically need to fill the supply gap. This also demonstrates that the increase in coal electricity had short-run benefits in terms of energy security and system reliability. The continued coal dispatch helped avoid more extreme outcomes, such as demand curtailment, blackout risk, or even higher electricity wholesale prices.

This study's findings also put the (short-term) effectiveness of a carbon price into perspective. Despite a high emission allowance price during the crisis, the exponential rise in gas prices rendered coal electricity generation more economical than gas. Our results provide insights into the required level of carbon pricing to deter a shift from gas to coal, thereby preventing an increase in emissions. While the average observed carbon price was 75 €/tCO₂ during the crisis, the hypothetical price would have been 2.6 times as high to avoid a switch from gas-to-coal.

While it is well understood that a carbon price can effectively reduce power-sector emissions in the short run via a fuel switch from coal to gas ([Gillingham and Stock, 2018](#); [Gugler et al., 2021, 2023](#); [Wilson and Staffell, 2018](#)), it remains open for debate whether a carbon price should reach such high levels as to prevent a gas-to-coal switch at all times. Similarly, studies from the U.S. have leveraged the fall in natural gas prices due to the hydraulic fracturing boom to infer the potential CO₂ abatement effect of a carbon price ([Cullen and Mansur, 2017](#); [Holladay and LaRiviere, 2017](#); [Knittel et al., 2019](#)). Moreover, a high carbon price that could have prevented the gas-to-coal switch might have caused energy security issues during the gas shortage ([Colgan et al., 2023](#)).

Hence, the results inform about the potential emission-abatement effects of a carbon price in other jurisdictions with a considerable coal-to-gas switching potential. Many electricity markets worldwide have similar supply structures, including substantial gas and coal generation capacities, as those observed in our dataset. Therefore, significant emissions reductions could be achieved short-term through a coal-to-gas switch. Our estimates also speak directly to policy design under stress.

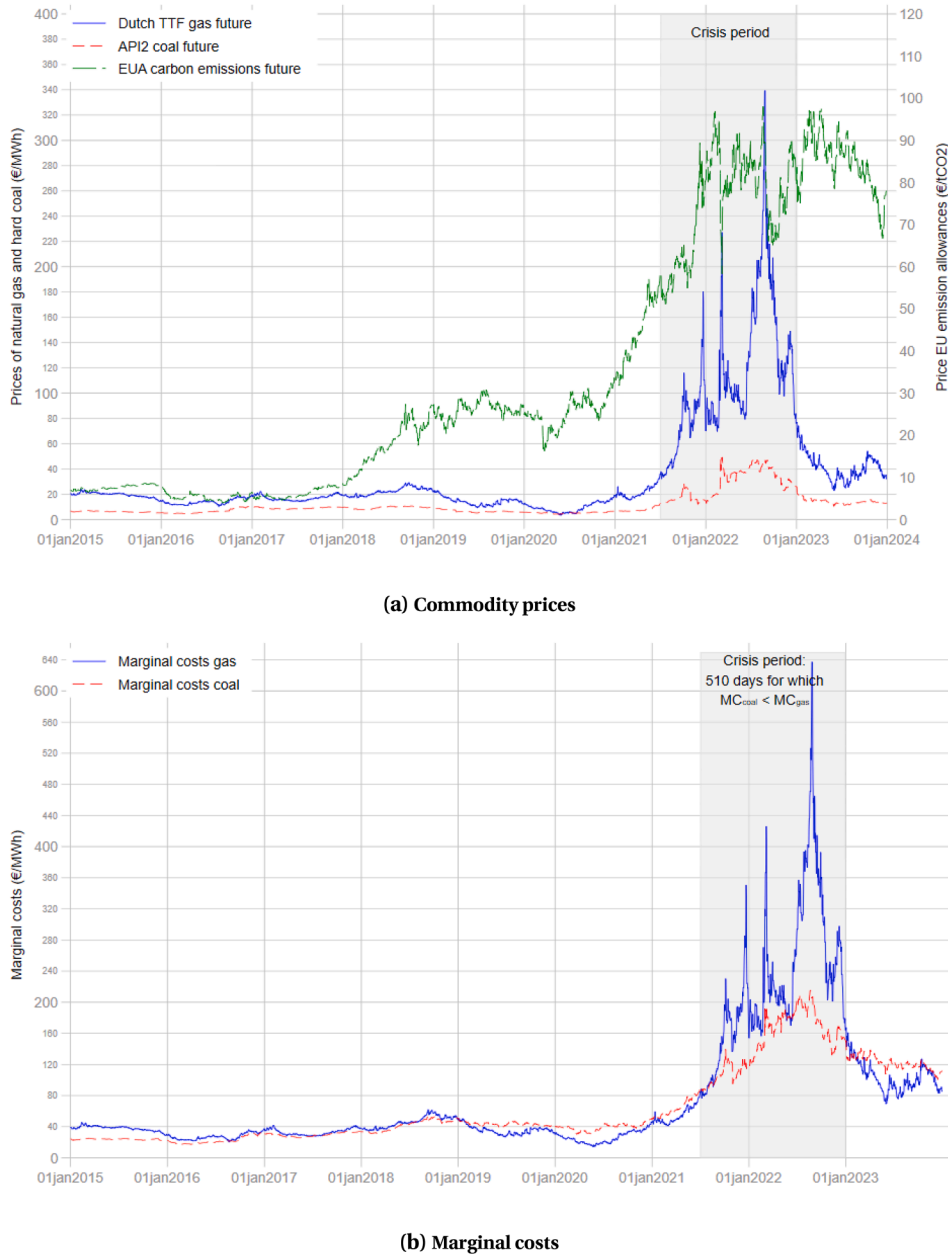


Fig. 1. Developments of prices and marginal costs. *This figure shows the developments of commodity prices and marginal costs for the daily frequency. In Fig. 1(b), the intersection between the marginal costs of coal and those of gas reflects a potential switching point.*

2. Marginal costs and gas-to-coal fuel switching

The aim of this study is to investigate the effect of a soaring gas price on coal-fired electricity production, local pollutants, and CO₂ emissions. That is, the gas price explosion changed the relative marginal costs of coal- and gas-fired electricity production, which likely prompted a gas-to-coal fuel switch in the merit order. Fig. 1(a) shows the trajectory of commodity prices throughout the study period. The price of gas started climbing mid-2021, followed by an explosion to 339 €/MWh on August 26, 2022. Coal prices experienced an uptick during the energy crisis, albeit to a lesser degree. Furthermore, reforms within the EU ETS prompted a rise in carbon allowance prices starting in late 2017, with a rapid escalation in 2021, reaching 98 €/tCO₂ on August 22, 2022.

The fluctuations in commodity prices are reflected in the evolution of the marginal costs associated with gas- and coal-fired electricity production. As depicted in Fig. 1(b), the costs of coal-generated electricity remained below those of gas until approximately the end of 2018. Subsequently, from 2019 to mid-2021, gas-generated electricity became more economical than coal, likely prompting

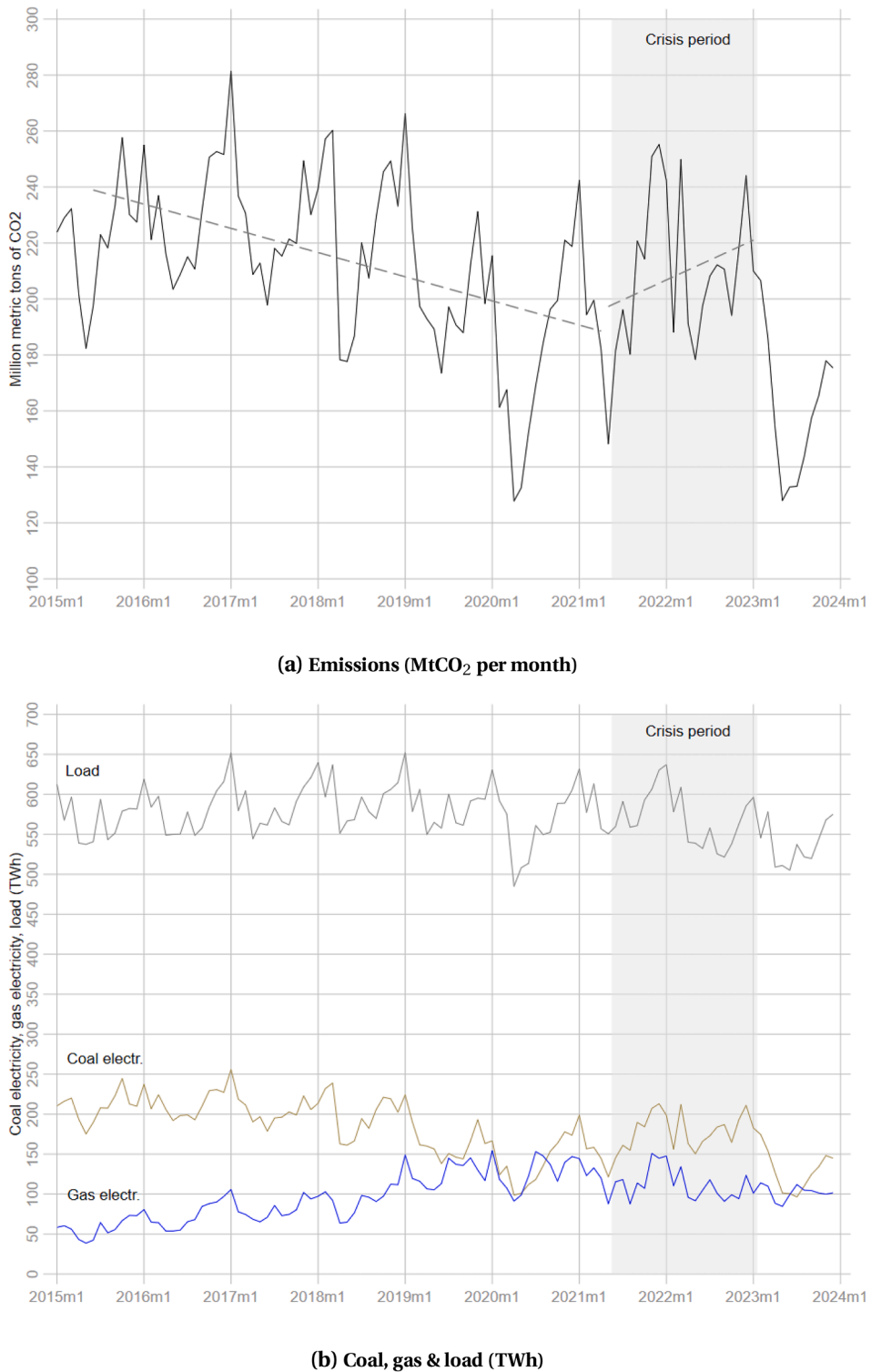


Fig. 2. Developments of emissions, electricity infeed from coal and gas, and load. *This figure depicts the trends of key variables, aggregated across the six sample countries and presented on a monthly basis. CO₂ emissions solely reflect those stemming from coal- and gas-based electricity generation. Coal electricity generation comprises lignite and hard coal. The data presented are observed (i.e., not modeled) and reflect actual measurements recorded over the specified period.*

a fuel switch between these two technologies. However, by mid-2021, the scenario shifted once more, with coal becoming cheaper throughout the energy crisis. Finally, during the crisis-recovery period in 2023, gas emerged as the cheaper supply technology most of the time. For the remainder of this study, we define the crisis period as the 510 days from July 1, 2021, to December 31, 2022, during which coal-fired electricity was cheaper than gas-fired electricity.

Moreover, Fig. 2(a) illustrates the trajectory of total coal- and gas-related CO₂ emissions for the six sample countries alongside local linear predictions for the pre-crisis and crisis periods. While emissions declined prior to the crisis, an upturn occurred during the crisis, which likely stems from a greater use of coal-fired electricity at the expense of less gas-fired electricity. This is initial descriptive evidence that the crisis prompted a gas-to-coal switch that increased emissions.

Fig. 2(b) supports this notion, showing that after a long period of narrowing coal- and gas-fired electricity production, the gap widened again significantly during the crisis period. Moreover, around the crisis period, a decrease in load can be observed, which likely contributed to a reduction in emissions. Hence, load is an important variable to control for in the econometric analysis.

3. Data

3.1. Selection of sample countries

Our empirical panel comprises Czechia, Germany, Ireland, Italy, the Netherlands, and Poland. These six EU countries satisfy two ex-ante rules, (i) a *Fuel-mix rule*: and (ii) a *policy-neutrality rule*. Rule (i) requires that the countries have a significant potential for gas-to-coal switching. Precisely, in 2019 both coal (lignite and hard coal) and gas nameplate capacity each had to exceed 10 % of average system load. This ensures that a relative-cost shock can move dispatch, as illustrated in Appendix Fig. A1.² Rule (ii) requires that during the 2021-22 energy crisis, none of the six countries imposed price-distorting measures, such as wholesale gas caps or fuel-specific carbon surcharges. Spain, Portugal, and Greece violated this rule by capping the wholesale gas price (EC, 2023). Moreover, Britain introduced a carbon tax on fossil-fuelled electricity production alongside the EU ETS allowance price in 2012 (Gugler et al., 2023), presenting a confounding policy factor that we are unable to disentangle, because it changes marginal costs independently of fuel prices. Furthermore, Britain's exit from the EU on February 1, 2020, introduced structural breaks, including the establishment of its own national emissions trading system and economic distortions, which confound our treatment period.

The retained countries together account for 64 % of EU-27 coal capacity, 57 % of gas capacity, and 62 % of coal-plus-gas electricity generation in 2020 (Eurostat, 2024; S&P Global, 2024). They cover northern, central, western, and eastern Europe and range from very large systems (Germany) to small ones (Ireland), so the sample is broadly representative of the European coal-gas landscape. Some Eastern European member states (e.g., Bulgaria, Romania, Hungary, Slovakia) fulfill rule (i), but lack continuous electricity market data (e.g., electricity generation by technology) for the full sample period (2015–2023), and are therefore omitted. The causal elasticity we estimate should transfer to other European countries that meet the same two rules, because the dispatch calculus is determined by identical relative-cost signals. Systems without a meaningful coal-gas margin are different: when gas prices rise, they cannot switch to coal and must rely on demand response, imports, nuclear, or renewables. In such settings, the short-run emission response to a gas price shock is likely weaker, and our point estimates would overstate the effect.

3.2. Data sources and calculations

We obtained publicly available data on the commodity prices of hard coal, natural gas, and carbon price from the financial market platform investing.com. For the price of natural gas, the daily closing price of the Dutch TTF one-month ahead future price from the Intercontinental Exchange (ICE) is used (investing.com, 2024c). The price of hard coal refers to the daily closing value of the API2 CIF ARA (ARGUS-McCloskey) one-month ahead coal future price (MTFc1) (investing.com, 2024b). For the carbon price, we obtained the daily closing value of EU emission allowances (EUA) (investing.com, 2024a). This price represents the value of an allowance certificate in Euros per metric ton of CO₂-equivalent, as determined within the European Union Emissions Trading System (EU ETS). We downloaded the data for the period January 1, 2015 to December 31, 2023 to match the electricity market data.

Aggregate country-level electricity production by technology and load are sourced from the publicly available (ENTSO-E, 2024) transparency platform. The retrieved data are available in 15-minutes or hourly frequency, depending on the year of publication. We aggregated the data to the daily frequency to match the variation in the commodity prices.

Coal-fired electricity production — Our primary dependent variable is coal-fired electricity production. We aggregated electricity production per day and per country from hard coal and lignite coal to obtain a measure of total coal-fired electricity production.

General notes on our approach to calculating emissions data — We study high-frequency variations using daily data. In our search for greenhouse gas and air pollution data, we explored several sources, including the EMEP Centre on Emission Inventories and Projections, which provides officially reported air pollution data by sector and EU country. However, we found these sources unsuitable for our study, as they typically report only annual data and for sectors that do not specifically focus on electricity generation.

² Many other European countries lack substantial capacity in either gas- or coal-fired generation. Including countries without coal capacity (e.g., France, Italy, Sweden) would add mostly zero observations on the dependent variable, pulling the estimated coefficients toward zero and offering little insight into the switching mechanism. Conversely, systems that possess coal capacity but no gas capacity cannot switch fuels, so their coal output would respond only weakly (if at all) to a gas-price shock.

As a result, we faced a trade-off: calculating CO₂ and local air pollution emissions specifically for the electricity generation sector and at a granular daily frequency using lignite-, hard coal-, and gas-fired generation data allows us to go beyond aggregate annual data analysis, though there may be estimation error compared with actual emissions.

Hence, we compute CO₂ and local air-pollution emissions mechanically from fuel-specific emission factors and efficiencies, independent of any health valuation. This implies that the results on CO₂, PM_{2.5}, NO_x, and SO₂ are direct outcomes of our causal coal-for-gas switching estimates. Yet, the estimation bias of our approach is likely small because we use high-frequency data that captures daily fuel use in electricity generation, allowing us to account for operational variations specific to lignite, hard coal, and gas plants. By applying capacity-weighted efficiency factors adjusted for fuel type, turbine technology, and vintage, we achieve emissions estimates closely aligned with actual plant performance. This targeted focus on electricity generation – unlike general inventories covering broader sectors – minimizes potential bias, resulting in more accurate sector-specific emissions calculations.

Efficiency factors — For the subsequent calculation of CO₂-equivalent emissions and marginal costs, efficiency factors are needed. An efficiency factor measures the ratio of electricity output (secondary energy) to fuel energy input (primary energy). It gives the percentage of the total energy content of a power plant's fuel that is converted into electricity.

We utilize the proprietary Platts PowerVision database by [S&P Global \(2024\)](#), which provides detailed information on all European power plants at the turbine level. This includes the country of location, unit online date (plant vintage), retirement date (if retired), primary fuel, primary turbine type, and nameplate capacity by year. We then apply efficiency factors according to turbine vintage, fuel type, and turbine type, using information provided by the Austrian Transmission System Operator, Austrian Power Grid (APG) (for a similar approach, see also [Gugler et al., 2020](#)). This approach allows us to construct capacity-weighted average efficiency factors by country, year, and fuel type.

While the initial Platts PowerVision data cannot be made available, we report the calculated efficiency factors. Appendix [Table A1](#) summarizes the efficiency factors that we apply, while Appendix [Table A2](#) provides a summary of the capacity-weighted efficiency factors per country, year, and fuel type in our sample. Our calculated efficiency factors are similar to typical efficiency factors per technology class reported in other sources (e.g., [UBA, 2022](#); [Quaschning, 2024](#)).

Marginal costs — We create a binary indicator, which equates one if the marginal costs of gas-fired electricity production exceed those of coal-fired electricity production.

Electricity dispatch can be approximated by a step-function supply curve, called the “merit order”. Plants bid typically their short-run marginal costs, and technologies enter in blocks. The key discontinuity for our question is whether gas or coal sits ahead in that order. We therefore create a binary indicator, which equates one if the marginal costs of gas-fired electricity production exceed those of coal-fired electricity production. This binary indicator variable is intended to mark the regime in which coal becomes cheaper than gas and is thus dispatched first. Small cost differences within a technology class (e.g., across vintages or efficiencies) create minor steps, but they do not alter the main coal-gas threshold. The indicator thus provides a parsimonious and economically meaningful proxy for the relevant kink in the supply curve.³

Following related studies ([Gugler et al., 2020, 2023](#)), we calculate the marginal costs (MC) as:

$$MC_{i,t,n} = \frac{p_{i,t,n} + \eta_n \cdot p_{CO2,t}}{\rho_{i,t,n}} \quad (1)$$

where i denotes the country, t denotes the sample day, n denotes the fuel type, $n = \{\text{hard coal, natural gas}\}$, p_n is the price of fuel $n = \{\text{hard coal, natural gas}\}$, p_{CO2} is the carbon price, η is the emissions factor per primary energy input (initially provided in g CO₂/kWh_{PE} and converted to tCO₂/MWh_{PE}). We set $\eta_{natural\ gas} = 0.2008$ and $\eta_{hard\ coal} = 0.3382$ ([IPCC, 2006](#); [UBA, 2022](#); [Quaschning, 2024](#)). ρ refers to the efficiency factor.⁴

The binary indicator is created as:

$$\mathbb{1}_{i,t} = \begin{cases} 1 & \text{if } (MC_{gas} > MC_{coal})_{i,t} \\ 0 & \text{otherwise} \end{cases} \quad (2)$$

This indicator variable measures for each day and each country if electricity production from natural gas is more expensive than that from coal.

CO₂-equivalent emissions Data — We calculated the CO₂-equivalent emissions from coal- and gas-fired electricity production, following ([Gugler et al., 2020, 2021, 2023](#)):

$$CO2_{i,t} = \sum_n \frac{g_{i,t,n} \cdot \eta_n}{\rho_{i,t,n}} \quad (3)$$

where i denotes the country, t denotes the sample day, n denotes the fuel type, $n = \{\text{lignite, hard coal, natural gas}\}$, g is electricity production, η is the emissions factor per primary energy input (in metric tons of CO₂ per MWh_{PE}) for a typical plant ([UBA, 2022](#); [IPCC, 2006](#)).

³ Robustness checks with the continuous marginal-cost spread in [Section 6](#) confirm that larger gaps add little once the switching threshold is crossed.

⁴ Note that a one-unit increase in a fuel price (P_{gas} or P_{coal}) maps into marginal costs via the inverse electric efficiency, i.e., $\partial MC_{gas}/\partial P_{gas} = 1/\rho_{gas}$ and $\partial MC_{coal}/\partial P_{coal} = 1/\rho_{coal}$. We use this scaling when translating level coefficients into an implied effect on the spread $S \equiv MC_{gas} - MC_{coal}$ in the robustness analysis ([Section 6](#)).

2006; Quaschning, 2024). Moreover, ρ refers to the efficiency factors calculated above. We set $\eta_{lignite} = 0.3987$, $\eta_{hardcoal} = 0.3382$, and $\eta_{naturalgas} = 0.2008$. We then aggregated the emissions from lignite coal and hard coal per day and per country to total coal-based CO₂ emissions.

Air pollution — We calculated local air pollution in kg of particulate matter (PM_{2.5}), nitrogen oxide (NO_x), and sulfur dioxide (SO₂), using latest available conversion factors to convert MWh of electricity infeed by fuel source (lignite coal, hard coal, natural gas):

$$Pollutant_{i,t,p} = \sum_n \frac{g_{i,t,n} \cdot \mu_{n,p}}{\omega} \quad (4)$$

where i denotes the country, t denotes the sample day, n denotes the fuel type, $n \in \{\text{lignite, hard coal, natural gas}\}$, p denotes the air pollutant, $p \in \{\text{PM}_{2.5}, \text{NO}_x, \text{SO}_2\}$, g is electricity production in MWh, μ is the emission factor in kg/TJ, and ω is a conversion factor from TJ to MWh (= 277.78). We set $\mu_{lignite,PM_{2.5}} = 0.78$, $\mu_{lignite,NO_x} = 70.83$, $\mu_{lignite,SO_2} = 240.3$ (UBA, 2019, Table 9), $\mu_{hardcoal,PM_{2.5}} = 1.15$, $\mu_{hardcoal,NO_x} = 55.63$, $\mu_{hardcoal,SO_2} = 36.85$ (UBA, 2019, Table 16), and $\mu_{naturalgas,PM_{2.5}} = 0.09$, $\mu_{naturalgas,NO_x} = 27.48$, $\mu_{naturalgas,SO_2} = 0.2$ (UBA, 2019, Tables 45 & 46). The reference source (UBA, 2019) pertains to Germany. Due to the absence of country-specific data, we assume that the other five European countries in our sample have similar emission factors.

Indicative health outcomes — The European Environment Agency (EEA, 2020)'s report on air quality in Europe states that “[a]ir pollution is a major cause of premature death and disease and is the single largest environmental health risk in Europe” (p. 10). It is, however, difficult to quantify premature deaths associated with fossil-fuelled electricity production given a lack of reliable data and causal identification strategies. We therefore convert coal-fired electricity production into indicative health outcomes using fuel-specific mortality factors from Markandya and Wilkinson (2007) and, for monetization, per-ton damage costs from EEA (2024). We emphasize that these are back-of-the-envelope implications rather than causal health estimates.

To our knowledge, Markandya and Wilkinson (2007) is the only published source that provides fuel-specific mortality factors suitable for translating the gas-to-coal switching we analyze into indicative estimates of premature deaths. The study quantifies the health effects of electricity generation in Europe, which also fits the scope of our analysis. According to this study, producing 1 TWh of electricity results in an estimated 32.6 premature deaths for lignite, 24.5 for hard coal, and 2.8 for natural gas, highlighting the substantial health burden associated with fossil fuel-based power generation. Moreover, 1 TWh of electricity causes 298 serious illnesses (including respiratory and cerebrovascular hospital admissions, congestive heart failure, and chronic bronchitis) for lignite, 225 for hard coal, and 30 for gas. These values pertain to air pollution and intentionally exclude power plant accidents.

The study dates back to 2007, implying that we have to assume that these estimates still apply for our study period. However, this concern is mitigated by the fact that many power plants operating in 2007 were still active during our sample period. Using the proprietary Platts PowerVision database by S&P Global (2024), we found that of the 2420 coal (hard coal & lignite) and gas power turbines built before 2007 and online as of January 1, 2007, 88 % (2,212 units) remained operational by January 1, 2023. Another limitation is that no country specific data are available. Despite these limitations, we utilize these values to quantify the premature deaths and serious illnesses related to our effect of interest. Hence, we transform electricity generation from coal and gas per sample day and per country into premature deaths and serious illnesses using these conversion factors.

As a cross-check, we compare our benchmark mortality factors from Markandya and Wilkinson (2007) with ratios implied by Jarvis et al. (2022). Using their reported fuel-specific changes in deaths and electricity generation by technology, we obtain indicative deaths per TWh of 24.8 for lignite, 32.5 for hard coal, and 7.9 for gas (see Appendix Table A3 for calculation details). While Jarvis et al. (2022) use German plants and exposure modeling (yielding higher gas values and a hard coal-to-lignite swap), the orders of magnitude align with Markandya and Wilkinson (2007) and confirm that coal's health burden per MWh far exceeds that of gas. We therefore retain Markandya and Wilkinson (2007) for transparency and comparability, emphasizing that our estimates are illustrative implications rather than observed health outcomes.

External health costs — We also assess the monetized external costs of air pollution through the combustion of fossil fuels on health. The European Environmental Agency (EEA, 2024, (page 26, Table 3.1)) provides marginal damages costs per local toxic air pollutant (PM_{2.5}, NO_x, and SO₂) for the year 2019. Specifically, these values are 237,123 EUR₂₀₂₁ per ton of PM_{2.5}, 42,953 EUR₂₀₂₁ per ton of NO_x, and 38,345 EUR₂₀₂₁ per ton of SO₂.

The damages primarily relate to health damages, but also incorporate damages to crops, forests, ecosystems & materials. The health damage values are presented for two different approaches, “value of a life year” (VOLY) and “value of statistical life” (VSL). According to EEA (2024, p. 10), VOLY is “an estimate of damage costs based on the potential years of life lost (YOLL) from a specific risk, based on an estimated life expectancy, and then evaluates them by multiplying them by the VOLY. Therefore, the result is affected by the age at which deaths occur.” On the other hand, VSL is “an estimate of damage costs based on the value a given population places ex ante on avoiding the death of an individual. VSL is based on the sum of money each individual is prepared to pay for a given reduction in the risk of premature death, for example from diseases linked to air pollution.” What is more, EEA (2024, (p. 22)) states that the “[o]pinion amongst economists is divided as to whether valuation is better represented by using the value of a life year (VOLY) or value of a statistical life (VSL).” Following Jarvis et al. (2022), we apply VSL values.

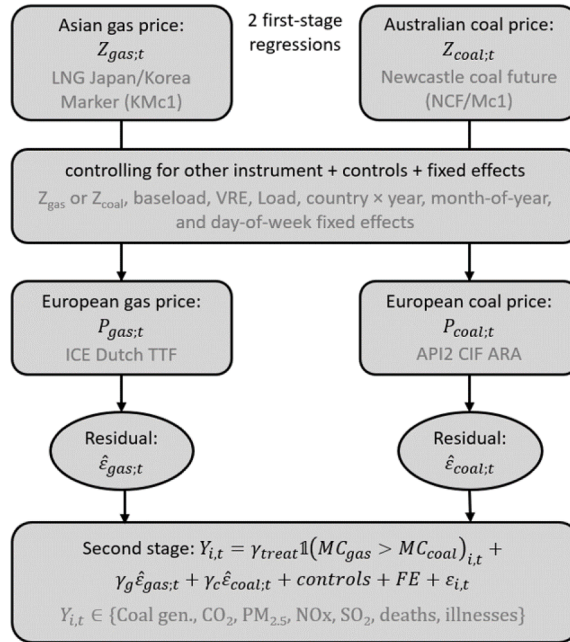


Fig. 3. Two-stage residual inclusion (2SRI) control-function approach. We run two separate first stages for the European gas and coal prices using external benchmarks as instruments, alongside controls and fixed effects, and obtain the fitted residuals $\hat{e}_{gas,t}$ and $\hat{e}_{coal,t}$. The second stage regresses $Y_{i,t}$ on the endogenous threshold $1(MC_{gas} > MC_{coal})_{i,t}$, the residuals $\hat{e}_{gas,t}$ and $\hat{e}_{coal,t}$, and the same controls + FE. The key econometric complication is that the potential endogeneity comes from the European fuel prices entering marginal costs, while the regressor of interest is a threshold $1(MC_{gas} > MC_{coal})$, i.e., a discontinuous nonlinear function of those prices. In such a setting, a control-function approach via the 2SRI estimator, which instruments the underlying prices and includes first-stage residuals, delivers a consistent estimate of γ_{treat} . The usual IV assumptions (instrument relevance and exclusion) apply.

4. Research design

4.1. Empirical strategy

We utilize an ex-post econometric model using daily historical data from January 1, 2015, to December 31, 2023. This model allows us to analyze increases in coal-fired electricity production in situations where the marginal costs of gas-fired generation exceed those of coal-fired generation, while controlling for other important confounding factors. In doing so, we capture the typical step-function shape of the electricity supply curve, which reflects dispatch decisions based on the marginal costs of different generation technologies.

To estimate the causal impact of a relative-cost shock – defined as days on which the marginal cost of gas-fired generation exceeds that of coal – on coal-fired electricity production and its environmental consequences, we employ a quasi-experimental model in the spirit of an instrumental variables estimator: a *two-stage residual inclusion (2SRI)* control-function approach (Terza et al., 2008; Wooldridge, 2015). This method is appropriate because the underlying European benchmark prices for natural gas and coal (ICE Dutch TTF and API2 CIF ARA) may respond endogenously to short-run supply and demand conditions.

In two first-stage regressions, we instrument each European benchmark fuel price with a corresponding benchmark price from other parts of the world: the LNG Japan/Korea Marker for gas (KMc1) (investing.com, 2024d) (henceforth referred to as the ‘Asian gas price’) and the Newcastle coal future (NCF/Mc1) for hard coal (investing.com, 2024e) (henceforth referred to as the ‘Australian coal price’). These contracts are traded on international exchanges and are orthogonal to daily shocks in European electricity dispatch, thereby satisfying the exclusion restriction. The fitted values from these first-stage regressions yield residuals that capture the endogenous component of domestic fuel prices. These residuals enter the second-stage equation alongside the observed switching indicator variable ($1(MC_{gas} > MC_{coal})$), rendering the latter conditionally exogenous. Fig. 3 visualizes the 2SRI approach.

The regression estimates allow for an interpretation of the additional coal-fired electricity produced in response to the gas price increase during the energy crisis. This is evaluated relative to a *counterfactual scenario* where the crisis did not occur and gas remained the cheaper option. We do this by comparing the actual treatment estimate relative to a coefficient estimate of zero (i.e., no treatment effect). Moreover, our regression estimates go beyond simple calculations of the emissions or deaths related to coal combustion, as they take the substitution between coal and gas electricity into account.

Data quality and variation play a key role for identification. We ensure high data quality through the use of reliable and publicly available sources, including the ENTSO-E transparency platform for electricity-market data and the financial platform investing.com

for commodity prices. Furthermore, our dataset exhibits significant variation on daily, monthly, seasonal, and yearly levels, both before and during crisis times, which we leverage for effect identification.

4.2. Econometric model

Choice of a binary switching indicator in our baseline regressions — Electricity dispatch follows a step-shaped merit order: when $MC_{gas} > MC_{coal}$, coal units move ahead of gas units in the queue and are dispatched first. Small intra-technology cost differences (e.g., unit vintage or efficiency) do not alter this discrete re-ordering. The indicator $\mathbb{1}(MC_{gas} > MC_{coal})$ therefore provides a parsimonious and economically meaningful summary of the regime shift we study.⁵

Naive structural specification — A regression that ignores endogeneity would model daily coal-fired generation ($Coal_{i,t}$) as a direct function of the switching indicator $\mathbb{1}(MC_{gas} > MC_{coal})_{i,t}$, which equals one when gas generation is more expensive than coal. Denoting the associated coefficient by β_{treat} , a fixed-effects panel specification for the six sample countries would read:

$$Coal_{i,t} = \beta_{treat} \mathbb{1}(MC_{gas} > MC_{coal})_{i,t} + \beta_B Baseload_{i,t} + \beta_V VRE_{i,t} + \beta_L Load_{i,t} + D_{i,y(t)} + D_{m(t)} + D_{d(t)} + \epsilon_{i,t} \quad (5)$$

where i indexes countries and t daily observations from 1 January 2015 to 31 December 2023. *Baseload* denotes baseload electricity infeed from nuclear and run-of-river power stations. *VRE* is electricity infeed from variable renewable energies, including onshore wind, offshore wind, and solar power. *Load* is electricity demand. The term $D_{i,y(t)}$ denotes country-by-year fixed effects, which absorb both all time-invariant country characteristics (e.g., topography, grid structure, climate conditions) and any country-specific shocks that change only once per year. $D_{m(t)}$ and $D_{d(t)}$ are month-of-year and day-of-week fixed effects, respectively. These temporal dummy variables account for seasonal cycles, as well as daily patterns that are not already captured by the previously mentioned control variables. They help control for factors such as technological advancements or learning rates, including fixed-cost degressions, within electricity production technologies. ϵ is a heteroskedasticity and autocorrelation-consistent (HAC) error term.

The switching indicator $\mathbb{1}(MC_{gas} > MC_{coal})_{i,t}$ is built from European benchmark fuel prices (ICE Dutch TTF and API2 CIF ARA); these prices may respond contemporaneously to regional demand shocks, strategic storage decisions, or policy announcements. If such shocks are also correlated with unobserved determinants of coal generation (e.g., plant outages, reserve margins, or short-run export constraints) then $\mathbb{1}(MC_{gas} > MC_{coal})_{i,t}$ is endogenous and OLS estimation of (5) yields a biased and inconsistent estimate of β_{treat} . To address this potential bias, we adopt a *two-stage residual inclusion* (2SRI) approach (Terza et al., 2008; Wooldridge, 2015).

Choice of 2SRI over 2SLS — For the potential threat of endogeneity in the European benchmark gas and coal prices ($P_{gas,t}$, $P_{coal,t}$), instrumentation is required. However, our regressor of interest is not the commodity price level itself, but a generated threshold variable, $D_{i,t} \equiv \mathbb{1}(MC_{gas} > MC_{coal})_{i,t}$, which is a discontinuous, nonlinear function of these benchmark prices. In this setting, a conventional 2SLS approach that replaces $D_{i,t}$ by its first-stage fitted value (or that constructs $D_{i,t}$ from fitted prices) generally does not recover the structural effect of crossing the coal-gas cost threshold, because it effectively instruments a nonlinear transformation via a linear projection. Control-function methods are designed for exactly this case: they instrument the underlying endogenous variables and then condition on the endogenous component through first-stage residuals (Terza et al., 2008; Wooldridge, 2015).

Accordingly, we first purge $P_{gas,t}$ and $P_{coal,t}$ using external instruments and then include the fitted residuals $\hat{\epsilon}_{gas,t}$ and $\hat{\epsilon}_{coal,t}$ in the second stage. Conditional on these residuals (and controls and fixed effects), the remaining variation in $D_{i,t}$ reflects exogenous shifts in the relative-cost ordering, so the coefficient on $D_{i,t}$ identifies the causal effect of the coal-ahead-of-gas regime.

2SRI approach — Each European benchmark fuel price is regressed on the instrumental variables, the Asian gas price and the Australian coal price, and on exogenous controls. The two first-stage regressions read:

$$P_{gas,t} = \pi_g Z_{gas,t} + \pi_c Z_{coal,t} + \alpha_{gas,B} Baseload_{i,t} + \alpha_{gas,V} VRE_{i,t} + \alpha_{gas,L} Load_{i,t} + D_{i,y(t)} + D_{m(t)} + D_{d(t)} + \epsilon_{gas,t} \quad (6a)$$

$$P_{coal,t} = \pi_g Z_{gas,t} + \pi_c Z_{coal,t} + \alpha_{coal,B} Baseload_{i,t} + \alpha_{coal,V} VRE_{i,t} + \alpha_{coal,L} Load_{i,t} + D_{i,y(t)} + D_{m(t)} + D_{d(t)} + \epsilon_{coal,t} \quad (6b)$$

where $Z_{gas,t}$ and $Z_{coal,t}$ are the Asian gas price and the Australian coal price, respectively. The fitted residuals are denoted $\hat{\epsilon}_{gas,t}$ and $\hat{\epsilon}_{coal,t}$, which are plugged into the second-stage regression to account for endogeneity.

Next, using European benchmark prices to construct the marginal-cost spread, coal-fired generation is modelled in the *second-stage regression*:

$$Coal_{i,t} = \gamma_{treat} \mathbb{1}(MC_{gas} > MC_{coal})_{i,t} + \gamma_g \hat{\epsilon}_{gas,t} + \gamma_c \hat{\epsilon}_{coal,t} + \gamma_B Baseload_{i,t} + \gamma_V VRE_{i,t} + \gamma_L Load_{i,t} + D_{i,y(t)} + D_{m(t)} + D_{d(t)} + \epsilon_{i,t} \quad (7)$$

If the critical IV assumptions of instrument relevance, exclusion restriction, and exogeneity of control variables are met (see Section 4.3), the parameter of interest, γ_{treat} yields a causal estimate of the effect of a gas-to-coal switch on coal-fired generation (Terza et al., 2008; Wooldridge, 2015).

⁵ In Section 6, we show that allowing for the magnitude of the spread $S \equiv MC_{gas} - MC_{coal}$ (linearly, quadratically, or by bins) yields positive but diminishing marginal effects once the threshold is crossed, corroborating the binary-switch specification as the main object of interest.

We estimate (7) with Newey-West standard errors (Bartlett kernel, lag 2) to accommodate heteroskedasticity and short-run autocorrelation. Log-specifications of the dependent variable are also reported so that $\beta_{treat} \cdot 100$ reads as a percentage change. Greenhouse-gas emissions, local air pollutants ($PM_{2.5}$, NO_x , SO_2) and health outcomes are analyzed by re-estimating (7) with those outcomes on the left-hand side, thereby capturing the gas-coal substitution directly in the regression framework.

For individual-country estimates, we adopt the model to a time-series framework:

$$Coal_t = \gamma_{treat} \mathbb{1}(MC_{gas} > MC_{coal})_t + \gamma_g \hat{\epsilon}_{gas,t} + \gamma_c \hat{\epsilon}_{coal,t} + \gamma_B Baseload_t + \gamma_V VRE_t + \gamma_L Load_t + D_{y(t)} + D_{m(t)} + D_{d(t)} + \epsilon_t, \quad (8)$$

which we estimate separately for each of the six countries.

Serial correlation and stationarity — Daily coal and gas prices, the dependent variables (e.g., coal-fired generation, CO_2 emissions), and control variables (baseload, VRE, load) are highly persistent. We address this in three ways: (i) we include rich fixed effects (country \times year, month-of-year, day-of-week) to absorb deterministic trends and seasonality; (ii) we use heteroskedasticity- and autocorrelation-consistent (HAC) standard errors with a 2-day bandwidth in the main tables; and (iii) we run unit-root tests on the fixed-effects-residualized series (Im-Pesaran-Shin panel tests for variables varying across countries (i) and time (t) and Augmented Dickey-Fuller tests for pure time-series variables), which indicate stationarity around the included fixed effects. These diagnostics suggest that our findings are not driven by spurious correlation arising from persistent trends.

4.3. Identifying assumptions

The two-stage residual-inclusion estimator is valid under three sets of conditions: *instrument relevance*, the *exclusion restriction*, and *exogeneity of controls*. Relevance is established empirically; exogeneity follows standard practice in the related power-sector literature (Cullen, 2013; Fell and Kaffine, 2018; Gugler et al., 2021). The exclusion restriction is discussed at greater length because it carries the main identifying content of the design.

Instrument relevance — Daily changes in the Asian gas price and the Australian coal price are strongly correlated with the European hub prices that feed the marginal-cost calculations through spatial arbitrage and expectations about arbitrage. The Kleibergen-Paap first-stage F statistic comfortably exceeds 10, satisfying the conventional rule-of-thumb for strong instruments (see Table 1).

Exclusion restriction — Conditional on the control variables and fixed effects, variations in the Asian and Australian benchmarks can influence European coal-fired generation only via their effect on the domestic marginal-cost spread.

Gas: The Asian benchmark gas price (the NG Japan/Korea Marker) is driven by Far-East LNG demand, Asian liquefaction outages, and Pacific freight rates. Physical LNG cannot move from the Pacific Basin to North-West Europe within the day, so a one-day shock to the Asian benchmark gas price cannot alter European dispatch by itself. Its effect is transmitted only through forward-curve arbitrage into the European gas price (the Dutch TTF) and hence into the marginal cost of gas-fired generation.

Coal: The Australian benchmark coal price (the Newcastle coal future NCF/Mc1) reflects Australian supply, Chinese import policy, and Panamax freight rates. Even at the peak of the 2021-22 energy crisis, extra European demand added less than one Panamax cargo per week to seaborne coal trade – far too small to affect a price set 15,000 km away at the Port of Newcastle. Conversely, any price shock at origin reaches European generators only after a shipping lag and therefore acts through delivered coal prices rather than directly on dispatch decisions.

Because the benchmark shocks originate in Asia-Pacific fundamentals and because European generators are price-takers on these markets, we treat the instruments as orthogonal to the structural error term in Eq. (7).

Exogeneity of controls — Electricity demand is effectively inelastic over a 24-hour horizon; the short-run price elasticity for Germany, for instance, is estimated at 0.05 (Hirth et al., 2024). Variable renewable output is weather-driven, and baseload generation from nuclear and run-of-river hydro is dispatched ahead of coal. These variables are therefore predetermined relative to daily fuel-price shocks. Carbon prices (EU ETS allowance futures) enter marginal-cost calculations but are set on a market whose daily variation is dominated by pan-European policy news and speculative trading. Individual countries' coal generation is too small to move the EUA price within a day, so the allowance price can be treated as exogenous at the country-day level, an assumption also made by Gugler et al. (2021). Country fixed effects absorb time-invariant heterogeneity such as topography or grid structure, while year, month-of-year, and day-of-week fixed effects capture macro-economic cycles, seasonal weather patterns, and systematic daily demand swings.

Implications — With strong, plausibly exogenous instruments and predetermined controls, coefficient γ_{treat} in Eq. (7) identifies the causal effect of a gas-to-coal switch on coal-fired generation. Re-estimating the same specification with CO_2 emissions, local pollutants, or health outcomes on the left-hand side then produces consistent estimates of the associated environmental and health impacts.

4.4. Counterfactual construction

Our impact estimates are obtained by contrasting observed outcomes on “switching” days with a model-based counterfactual in which gas remained cheaper than coal. Formally, $\mathbb{1}(MC_{gas} > MC_{coal})_{i,t}$ indicates if gas is more expensive than coal in country i on day t . Eq. (7) yields the treatment coefficient γ_{treat} from the 2SRI regression. The counterfactual outcome for country i and day t is then

$$Y_{it}^{cf} = \hat{Y}_{it} - \gamma_{treat} \cdot \mathbb{1}(MC_{gas} > MC_{coal})_{i,t}. \quad (9)$$

Table 1
Two-stage residual inclusion (2SRI): first stages & second stage.

	(1) 1st stage Coal price	(2) 1st stage Gas price	(3) 2nd stage Coal gen.
Austr. coal price	0.482*** (0.00907)	0.749*** (0.0355)	
Asian gas price	0.247*** (0.00596)	3.256*** (0.0449)	
$\mathbb{1}(MC_{gas} > MC_{coal})$			17420.5*** (1674.4)
$\hat{\epsilon}_{coal}$			-231.6 (176.2)
$\hat{\epsilon}_{gas}$			77.01* (39.85)
Baseload	-0.00000165*** (0.000000642)	0.00000562** (0.00000253)	-0.0363 (0.0272)
Load	0.000000810*** (0.000000240)	-0.000000141 (0.000000984)	0.427*** (0.00920)
VRE	7.08e-08 (0.000000210)	-0.00000300*** (0.000000834)	-0.462*** (0.00685)
Country×Year FE	yes	yes	yes
Month FE	yes	yes	yes
Day-of-week FE	yes	yes	yes
Observations	19,363	19,363	19,322
R-squared	0.952	0.958	0.955
K.P. first-stage F			504

Notes: $\hat{\epsilon}_{coal,i,t}$ and $\hat{\epsilon}_{gas,i,t}$ are the fitted residuals from the first-stage regressions. “K.P.” denotes the Kleibergen-Paap rk Wald F statistic for instrument relevance. HAC (Newey-West, $bw = 2$) standard errors in parentheses. Significance: * $p < 0.10$, ** $p < 0.05$, *** $p < 0.01$.

That is, we set the switching indicator to zero while holding all other covariates (including the fixed effects and residual corrections) at their observed values.⁶ Aggregating over countries and days gives the total effect:

$$\Delta Y = \sum_i \sum_t \gamma_{\text{treat}} \cdot \mathbb{1}(MC_{gas} > MC_{coal})_{i,t}. \quad (10)$$

This counterfactual is valid if, conditional on our controls, no other major shocks systematically affect coal generation on switching days except the relative marginal costs of coal and gas (captured by $\mathbb{1}(MC_{gas} > MC_{coal})_{i,t}$). We also assume that the estimated regression relationship is stable (structural invariance). Under these conditions, we construct the counterfactual by “turning off” the price-switch indicator (setting $\mathbb{1}(MC_{gas} > MC_{coal})_{i,t} = 0$) while keeping all other variables at their observed values. However, this counterfactual analysis does not capture adaptive behavior beyond what the controls reflect, such as accelerated renewable build-out, structural (rather than short-run) demand adjustments, or strategic storage investments. Such longer-term responses are outside the scope of this study and remain a task for future research.

5. Results

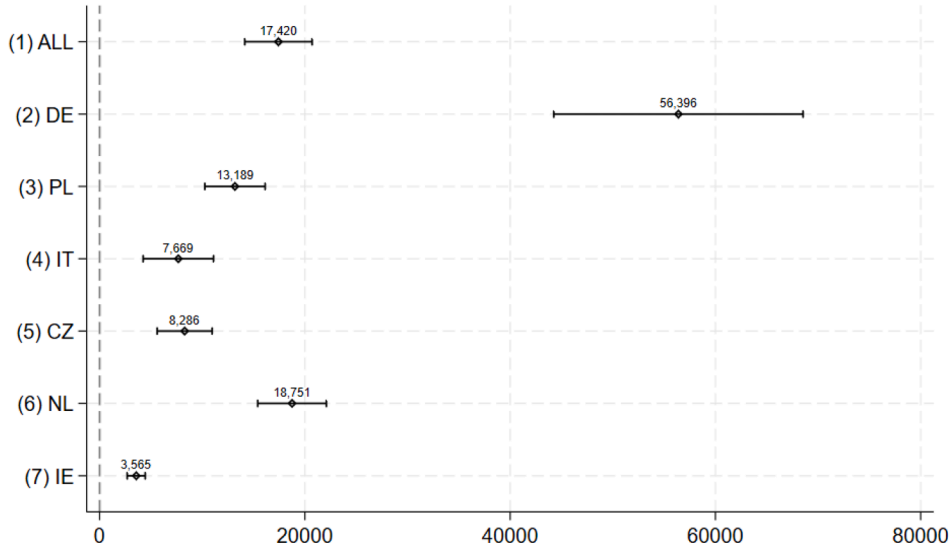
This section first contrasts 2SRI with naive OLS estimates. It then shows that the gas price surge drove a marked rise in coal generation, CO₂ emissions, local air pollution, health outcomes, and related monetary health costs.

Performance of 2SRI — Table 1 reports the first-stage price equations (columns 1–2), the second-stage control-function (2SRI) regression (column 3). As expected, the excluded instruments (Asian gas price, Australian coal price) are highly predictive of the corresponding European benchmark prices. The reported Kleibergen-Paap rk Wald F statistic of 504 (joint test of excluded instruments across endogenous regressors) comfortably exceeds the conventional weak-instrument rule-of-thumb threshold of 10, indicating strong instruments.

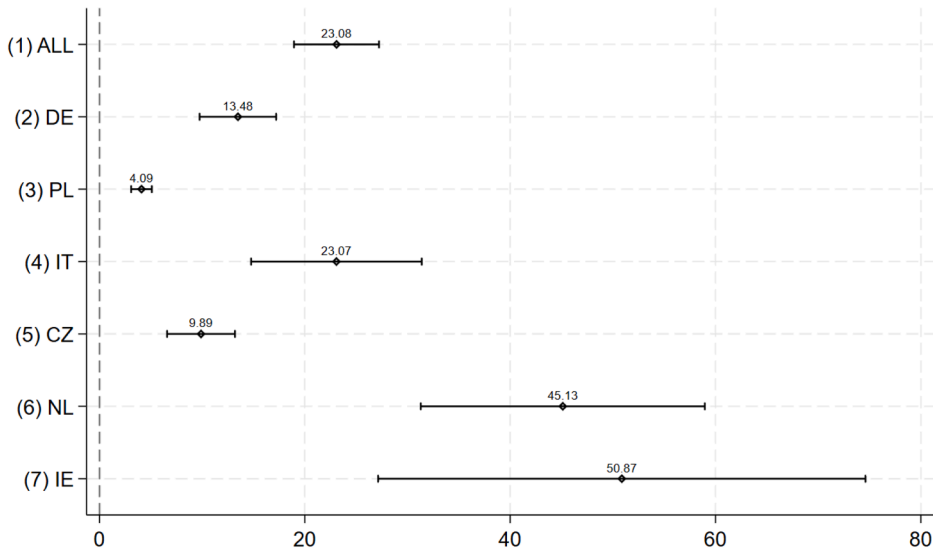
In the second stage, the residual from the first-stage gas price regression ($\hat{\epsilon}_{gas}$) is statistically significant at the 10 % level, while the residual from the coal price regression ($\hat{\epsilon}_{coal}$) is not. This pattern indicates that endogeneity arises primarily through the gas price. Conditional on the included controls and fixed effects, coal price variations do not display detectable correlation with the outcome error term. Hence, the control-function (2SRI) adjustment is warranted mainly to purge gas-price-driven endogeneity.

Overall, instrument strength is high, endogeneity appears limited to the gas price channel, and the corrective 2SRI procedure produces a treatment effect estimate that is likely unbiased. In what follows, we focus on the 2SRI estimates as our preferred causal

⁶ Equivalently, one can predict \tilde{Y}_{it} from the estimated model with $\mathbb{1}(MC_{gas} > MC_{coal})_{i,t} = 0$ and then aggregate $\Delta Y_{it} = \hat{Y}_{it} - \tilde{Y}_{it} = \gamma_{\text{treat}} \cdot \mathbb{1}(MC_{gas} > MC_{coal})_{i,t}$.



(a) Absolute effect on coal electricity infeed (MWh per day)



(b) Relative (logarithmic) effect on coal electricity infeed (%)

Fig. 4. Increase in coal-fired electricity production. *Fig. 4(a)* depicts the coefficient estimates for $\mathbb{1}(MC_{\text{gas}} > MC_{\text{coal}})$, including 95 % confidence intervals. These estimates represent the change in coal-fired electricity generation per day when coal-generated electricity is cheaper than gas-generated electricity. *Fig. 4(b)* shows the relative effects derived from a regression where $\log(\text{emissions})$ serves as the dependent variable. The coefficients have been multiplied by 100 to represent percentage values. “All” refers to a panel regression of all six countries, which includes country fixed effects.

results and discuss their economic magnitude regarding coal-fired electricity generation, associated CO₂ emissions, local air pollution, and related health outcomes.

Increased coal-fired electricity — *Fig. 4(a)* plots the estimated effect of a relative-cost shock ($\mathbb{1}(MC_{\text{gas}} > MC_{\text{coal}}) = 1$) on coal-fired generation. As hypothesized, coal output rises on days when the marginal costs of gas exceed those of coal. The six-country panel specification yields an average increase of 17,420 MWh of coal-generated electricity per country-day when coal is cheaper than gas. During the energy crisis period from 1 July 2021 until 31 December 2022, there were 510 calendar days on which coal generation was cheaper than gas. All else equal, this suggests that the energy crisis resulted in an increase of 53 TWh ($\approx 17,420 \text{ MWh} \cdot 510 \text{ days} \cdot 6 \text{ countries}$) (95 % CI: 43–63 TWh) of coal-fired electricity production across the six countries under investigation. However, country-

level heterogeneity is substantive. Germany exhibits the largest absolute response: 56,396 MWh (95 % CI: 44,250–68,541 MWh) of additional coal generation per switching day. The Netherlands shows 18,751 MWh (95 % CI: 15,407–22,095 MWh), while Ireland's effect is 3,565 MWh (95 % CI: 2,686–4,443 MWh). Smaller absolute effects in some countries reflect both more limited installed coal capacity and a lower baseline coal share.

Fig. 4(b) reports effects in relative terms. On average, across the sample, coal-fired generation increased by 23 % per switching day. The relative effect is largest in Ireland (51 %), reflecting a small baseline coal level, and smallest in Poland (4 %), where the pre-existing coal share is high. Relative (percentage) effects highlight the intensity of gas-to-coal switching potential within each system, whereas absolute (MWh) effects also scale with system size and therefore are more informative for downstream impacts on CO₂ and local air pollutant emissions. These absolute increments underpin the emission, air quality, and health impact estimates discussed below.

Heightened CO₂ emissions — **Fig. 5** displays the absolute (levels) and relative (percentage) responses of CO₂ emissions to a relative-cost shock. According to the panel specification, emissions increase by 11,891 tCO₂ per country-day when coal is cheaper than gas (Specification 1, **Fig. 5(a)**). Over the energy-crisis window, with 510 days on which coal was cheaper than gas, this resulted in 36 Mt of additional CO₂ emissions ($\approx 11,891 \text{ t} \cdot 510 \text{ days} \cdot 6 \text{ countries}$) (95 % CI: 28–45 Mt), relative to the counterfactual scenario in which gas remained the cheaper fuel.

Applying the latest available central estimate of the social cost of carbon of 180 USD₂₀₂₀ ($\approx 158 \text{ EUR}_{2020}$) per tCO₂ (Rennert et al., 2022) yields an associated global damage cost of about 6.55 billion USD₂₀₂₀ ($\approx 5.73 \text{ billion EUR}_{2020}$). These costs proxy the present value of incremental climate damages (or equivalently, the benefit of counterfactual abatement).

Country heterogeneity is substantial. Germany exhibits the largest absolute response (38,056 tCO₂ per switching day, 95 % CI: 27,020–49,092 t). Other countries experienced a less pronounced absolute effect, varying between 12,696 tCO₂ (95 % CI: 9,840–15,552 t) in Poland and 3524 tCO₂ (95 % CI: 2,550–4,498 t) in Ireland.

In relative terms, CO₂ emissions increased by 10 % across the six sample countries on switching days. The elasticity is highest for Ireland (26 %), where the small baseline makes percentage swings large, and lowest (and statistically insignificant) for Italy (0.4 %). **Increased air pollution** — The literature documents that coal-fired electricity generation emits more particulate matter, heavy metals, sulfur dioxide, and nitrogen oxides than any other source of electricity (Hendryx et al., 2020; Barreira et al., 2017). The release of these toxic air pollutants has well-established adverse health effects, including a significantly higher mortality risk (Henneman et al., 2023; Jerrett, 2015; Geng et al., 2021; Carugno et al., 2016), increased infant mortality (Chay and Greenstone, 2003), more outpatient visits and higher medical expenses (Zheng et al., 2023), reduced life satisfaction and well-being (Petroski et al., 2021; Wang et al., 2025), and a marked rise in respiratory and cardiovascular diseases (Honscha et al., 2021; Burt et al., 2013), including asthma (McCarron et al., 2023) and other pulmonary illnesses (Moore et al., 2016).

In addition, a growing body of research highlights both immediate and longer-term negative effects of air pollution on cognitive and physical performance. Documented impacts include declines in verbal and math test scores (Zhang et al., 2018; Duque and Gilraine, 2022), lower university entrance exam results (Carneiro et al., 2021), deteriorating mental health (Xue et al., 2019; Ren et al., 2019), increased criminal behavior (Bondy et al., 2020; Herrnstadt et al., 2021; Cruz et al., 2022), reduced worker productivity (Chang et al., 2019), and diminished soccer performance (interpreted as individual productivity; Licher et al., 2017). These findings underscore the importance of understanding the rise in air pollutants and premature deaths associated with the gas-to-coal shift during the energy crisis.

Fig. 6 presents panel regression estimates on the increase in PM_{2.5}, NO_x, and SO₂ per day and per country whenever gas is more expensive than coal. Local air pollution increases significantly due to intensified coal-fired electricity production relative to the counterfactual scenario in which gas remained the cheaper fuel. During the 510 crisis days when gas was more expensive than coal, PM_{2.5} increased by 187 t ($\approx 61.13 \text{ kg} \cdot 510 \cdot 6$) (95 % CI: 152–222 t) or 19 %, NO_x by 8645 t ($\approx 2825 \text{ kg} \cdot 510 \cdot 6$) (95 % CI: 6,573–10,715 t) or 10 %, and SO₂ by 16,303 t ($\approx 5328 \text{ kg} \cdot 510 \cdot 6$) (95 % CI: 10,947–21,658 t) or 24 %.

Additional indicative health impacts — We provide an *illustrative* quantification of potential health impacts associated with the gas-for-coal switching episodes. Using exogenous benchmark damage factors from Markandya and Wilkinson (2007) for premature deaths and serious illnesses attributable to combustion of lignite, hard coal, and natural gas in Europe, we estimate substantial increases linked to the fuel switch. **Fig. 7** presents panel regression estimates at the country-day level for periods when natural gas was more expensive than coal. We find approximately 1285 ($\approx 0.42 \cdot 510 \cdot 6$) (95 % CI: 1,022–1,567) additional premature deaths and 11,781 ($\approx 3.85 \cdot 510 \cdot 6$) (95 % CI: 9,285–14,256) cases of serious illnesses, corresponding to roughly a 17 % relative increase in each outcome.

These figures should be interpreted strictly as indicative orders of magnitude rather than refined epidemiological estimates. The Markandya and Wilkinson (2007) study is widely cited, fuel-comparable, and transparent, which facilitates a reproducible back-of-the-envelope translation from additional coal generation to plausible health burdens. This transparency helps readers gauge potential welfare stakes of the fuel switch. However, these indicative estimates inherit limitations from using static literature-based factors rather than contemporaneous emission inventories and concentration-response modeling. For example, they omit more recent plant upgrades that probably reduced marginal emissions, ignore medical advances, and disregard any changes in population density gradients. We therefore present these estimates solely as indicative health-outcome effects to contextualize the welfare relevance of the coal displacement effect. A full health impact assessment (e.g., integrating plant-level emission factors, atmospheric dispersion modeling, and current concentration-response functions) is beyond the scope of this paper.

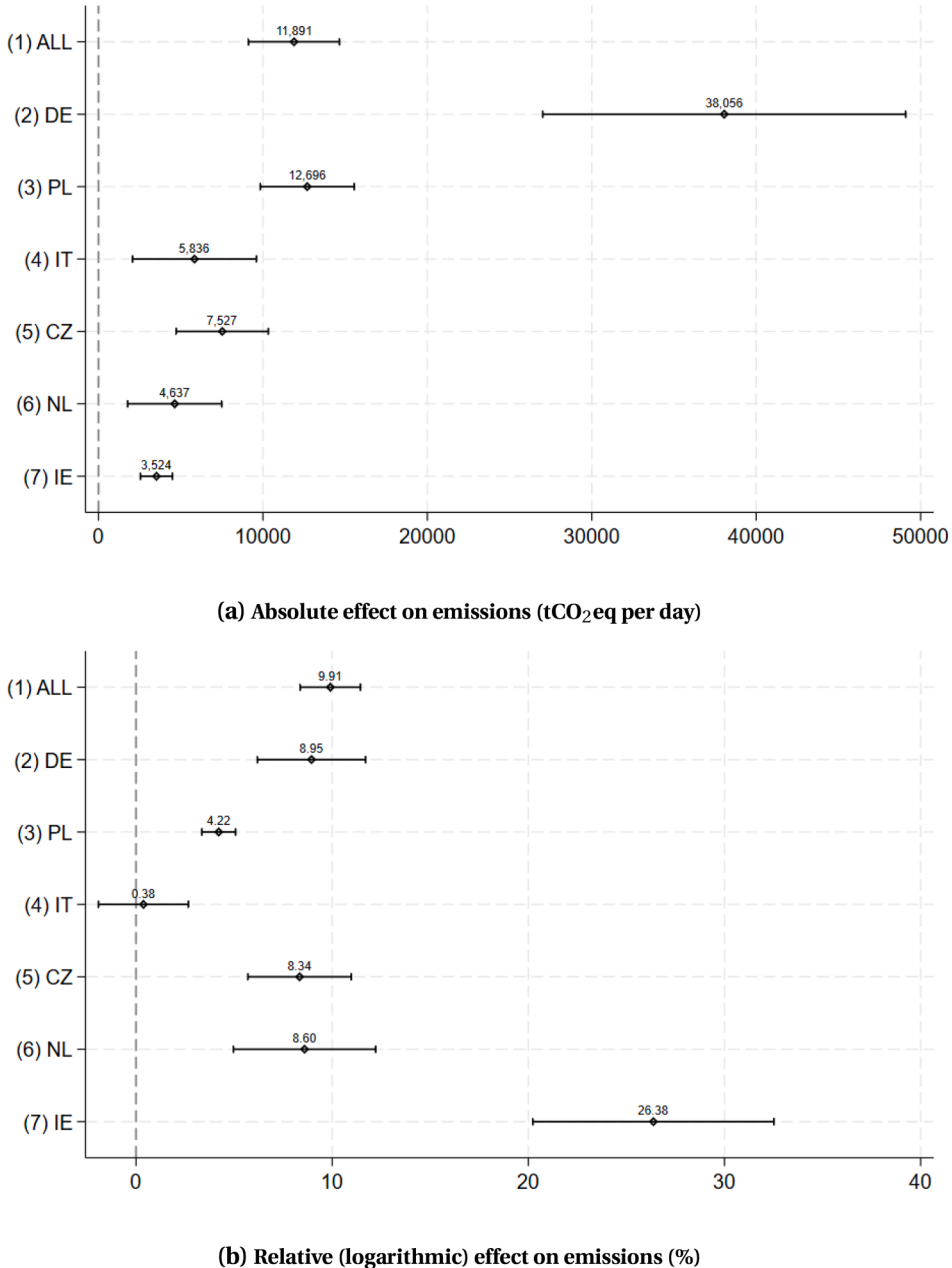


Fig. 5. Increase in CO₂-equivalent emissions. **Fig. 5(a)** depicts the coefficient estimates for $\mathbb{1}(MC_{\text{gas}} > MC_{\text{coal}})$, including 95 % confidence intervals. These estimates signify the alteration in tons of CO₂ per day when coal-generated electricity is cheaper than gas-generated electricity. **Fig. 5(b)** depicts the relative effects derived from a regression where $\log(\text{emissions})$ serves as the dependent variable. The coefficients have been multiplied by 100 to represent percentage values. “All” refers to a panel regression of all 6 countries, which includes country fixed effects.

Elevated external health costs — Moreover, to assess the external health damage costs of the increase in air pollution, we apply estimates expressed in monetary values (EUR₂₀₂₁) by the European Environmental Agency (EEA, 2024): 237,123 EUR₂₀₂₁ per ton of PM_{2,5}, 42,953 EUR₂₀₂₁ per ton of NO_x, and 38,345 EUR₂₀₂₁ per ton of SO₂. Our findings of an additional 187 t PM_{2,5}, 8645 t NO_x, and 16,304 t SO₂ thus translate to 44,342,001 EUR₂₀₂₁ for PM_{2,5}, 371,328,685 EUR₂₀₂₁ for NO_x, and 625,176,880 EUR₂₀₂₁ for SO₂. This makes a total of 1.04 billion EUR₂₀₂₁ of external damage costs related to the air pollution caused by the energy crisis.

These effects indicate a pronounced increase in local air pollution, with significant adverse health effects, particularly in the form of premature deaths. Moreover, there may have been other severe adverse impacts on human health, cognitive abilities, and physical performance, which we could not quantify for a lack of available data. Overall, this points to significant economic costs of the crisis

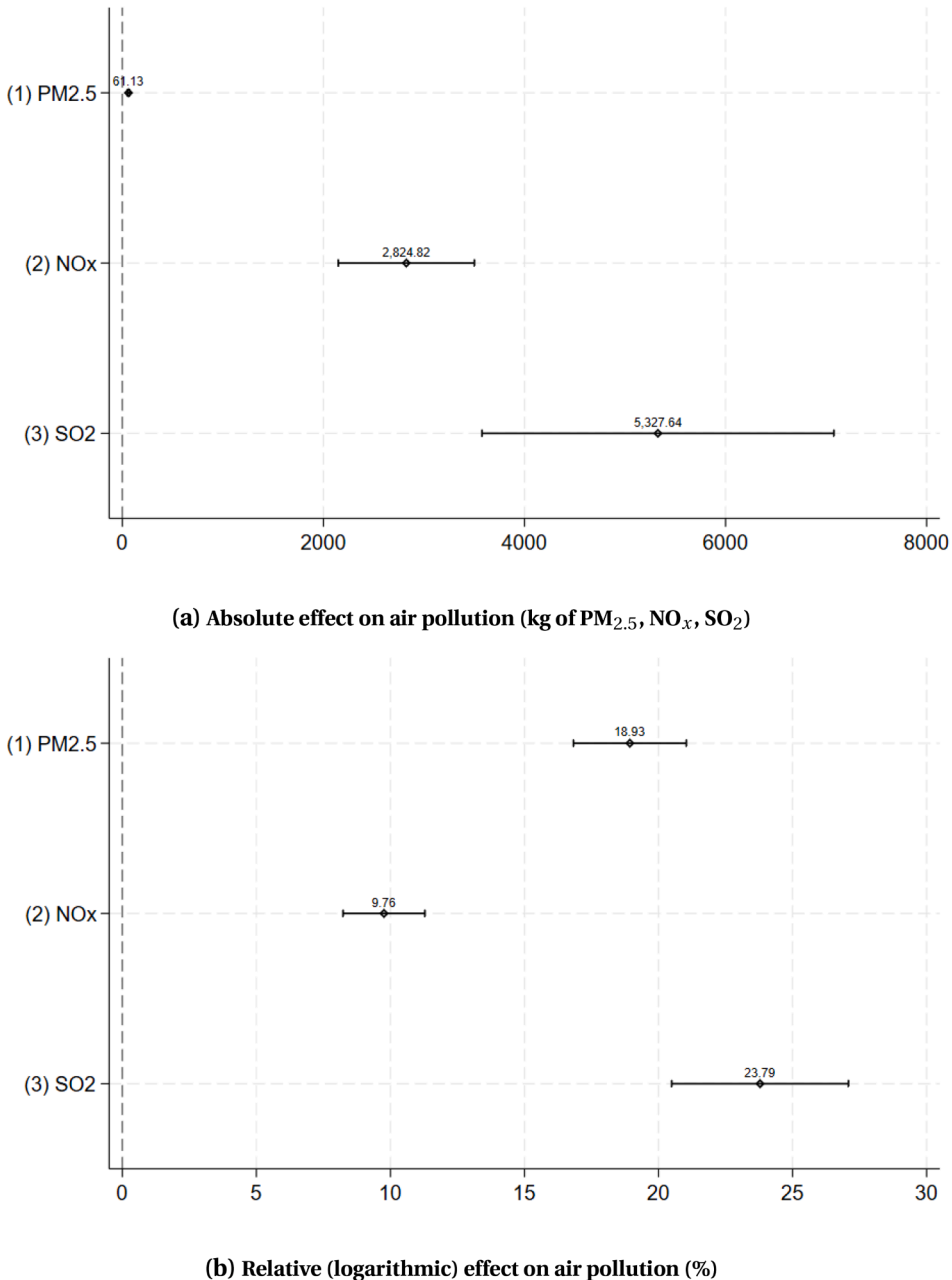
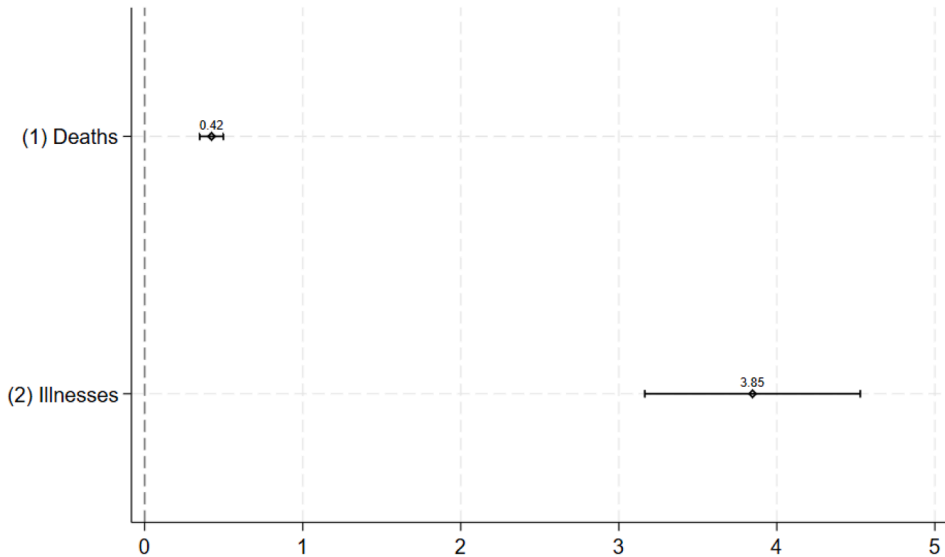


Fig. 6. Increase in PM_{2.5}, NO_x, and SO₂. **Fig. 6(a)** depicts the coefficient estimates for $\mathbb{1}(MC_{\text{gas}} > MC_{\text{coal}})$, including 95 % confidence intervals, from panel regressions of all 6 countries including country fixed effects. These estimates signify the change in kg of PM_{2.5}, NO_x, and SO₂ per day per country when coal-generated electricity is cheaper than gas-generated electricity. **Fig. 6(b)** depicts the relative effects derived from a regression where all dependent variables are logarithmized. The coefficients have been multiplied by 100 to represent percentage values.

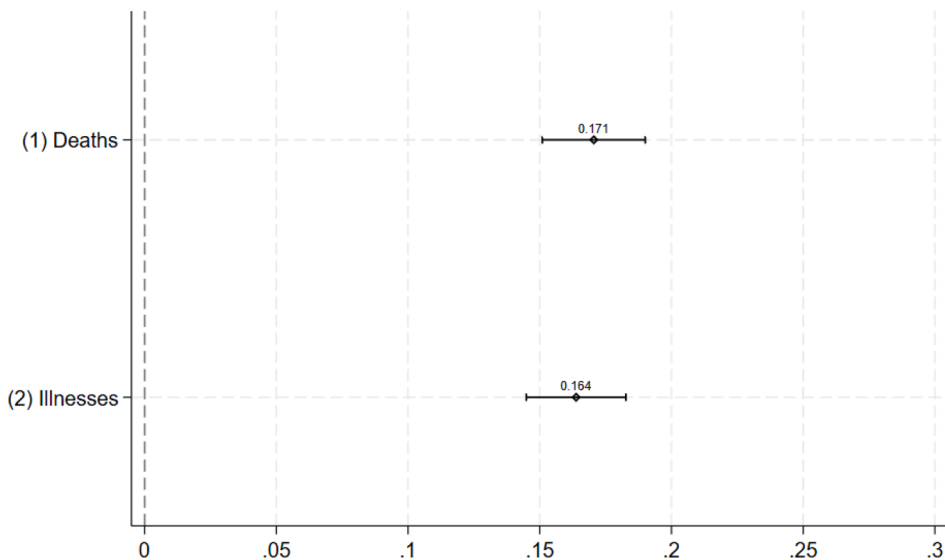
due to an increased burning of coal. Our estimates indicate that the additional external damage costs are enormous, exceeding one billion Euros.

Hypothetical carbon price to avert gas-to-coal switching — Finally, we construct for each crisis day a *hypothetical* carbon price that would remove any economic incentive to dispatch coal ahead of gas, even at the peak gas prices observed (up to 339 €/MWh). Concretely, we set the marginal cost of gas-fired generation equal to that of coal-fired generation, $MC_{\text{gas}} = MC_{\text{coal}}$, in Eq. (1) and solve for the carbon price that fulfills this condition:

$$\frac{p_{\text{coal};t} + \eta_{\text{coal}} \cdot p_{\text{CO2};t}}{\rho_{\text{coal}}} = \frac{p_{\text{gas};t} + \eta_{\text{gas}} \cdot p_{\text{CO2};t}}{\rho_{\text{gas}}},$$



(a) Absolute effect on premature deaths and serious illnesses (# of deaths, # of cases)



(b) Relative (logarithmic) effect on premature deaths and serious illnesses (%)

Fig. 7. Increase in premature deaths and serious illnesses. **Fig. 7(a)** depicts the coefficient estimates for $\mathbb{1}(MC_{gas} > MC_{coal})$, including 95 % confidence intervals, from panel regressions of all 6 countries including country fixed effects. These estimates signify the change in cases of deaths and illnesses per day per country when coal-generated electricity is cheaper than gas-generated electricity. **Fig. 7(b)** depicts the relative effects derived from a regression where all dependent variables are logarithmized. The coefficients have been multiplied by 100 to represent percentage values.

following Eq. (1). We then solve for the carbon price:

$$p_{hypCO2,t} = \frac{\rho_{coal}p_{gas,t} - \rho_{gas}p_{coal,t}}{\eta_{coal}\rho_{gas} - \eta_{gas}\rho_{coal}} \quad (11)$$

This back-of-the-envelope exercise illustrates the potential emissions (and associated damage cost) savings that a sufficiently high carbon price could have delivered by preventing coal displacement of gas.

Fig. 8 juxtaposes the observed EUA allowance price with the implied hypothetical price. To suppress coal switching even at the peak gas price observed during the crisis, the carbon price would have needed to rise to roughly 760 €/tCO₂. Over the full crisis

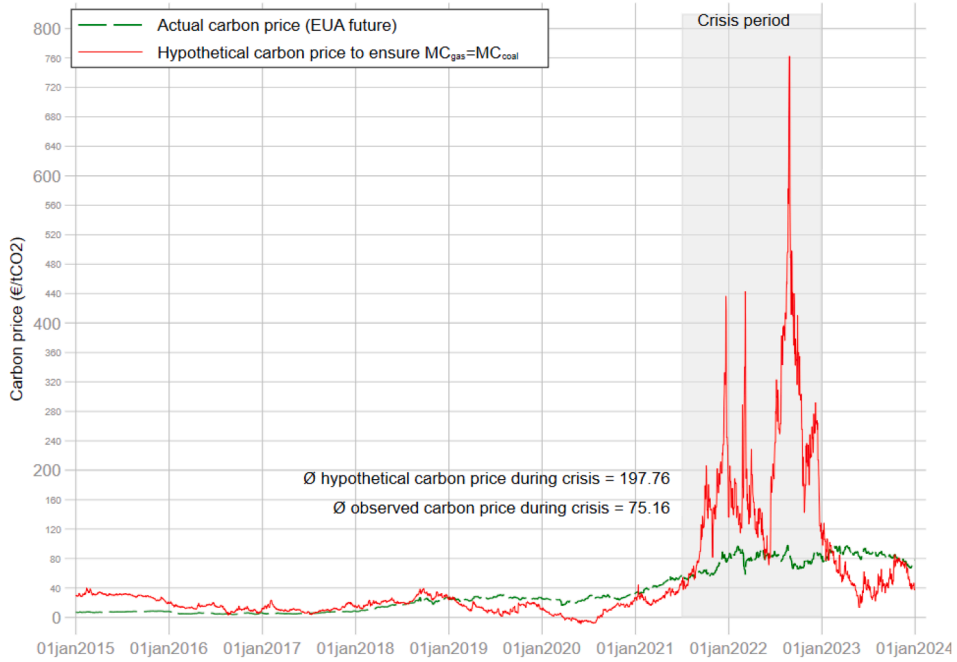


Fig. 8. Actual carbon price vs. hypothetical carbon price to avoid a fuel switch ($MC_{gas} = MC_{coal}$).

window, the average observed EUA price was about 75 €/tCO₂, whereas the average hypothetical no-switch price is approximately 198 €/tCO₂ – about 2.6 times higher.

Economic context and trade-offs — Our estimates quantify the environmental and health costs of gas-for-coal switching induced by a relative fuel price shock. They do not, however, deny that this switch may have conveyed short-run benefits in terms of energy security and system reliability. In the face of sharply higher gas prices and constrained supply, continued coal dispatch helped avoid more extreme outcomes: demand rationing, blackout risk, or even higher wholesale prices, with potentially drastic economic consequences. From a cost-benefit perspective, the external damages we report (CO₂, local pollution, health) are one side of the ledger; the benefits in the form of avoided outage costs, reduced value of lost load, and lower geopolitical exposure are the other. While our data do not allow us to monetize these benefits rigorously, acknowledging this trade-off situates our findings within a broader welfare framework. Future research could integrate plant-level dispatch models with estimates of outage costs or security-of-supply metrics to quantify the net welfare impact more fully.

ETS cap, waterbed, and short-run welfare — The welfare interpretation of our CO₂ results within the EU ETS hinges on whether the cap is effectively fixed or partially state-contingent. Under a fixed cap, the classic waterbed effect applies: additional emissions in the power sector raise allowance demand and prices but do not change cumulative emissions for a fixed supply of CO₂ certificates, so the climate externality is shifted intertemporally or across sectors rather than increased in total (Rosendahl, 2019). Since Phase 4, however, the Market Stability Reserve (MSR) partly punctures the waterbed by adjusting future auction volumes in response to the previous year's total number of allowances in circulation and by invalidating surplus allowances once the reserve exceeds a threshold (Perino, 2018; ICAP, 2024; UBA, 2022). These adjustments are annual and backward-looking (based on prior-year total allowances in circulation), i.e., they do not smooth day-to-day shocks from commodity-price spikes. Thus, for our short-run daily dispatch effects during the crisis, the classic waterbed intuition remains a good approximation, while over longer horizons the MSR can lower cumulative emissions via invalidation. Importantly, our results remain directly policy-relevant for (i) national and sectoral CO₂ targets outside the EU-wide cap accounting and (ii) local air pollutants and health damages, which lie outside the ETS and therefore are not offset by the cap.

Uncertainties and limitations — Our estimates carry several sources of uncertainty. For example, we are estimating short-term changes in coal-fired electricity production and related CO₂, pollution, and health outcomes, whereas we are unable to model longer-term structural adjustments or adaptive behaviors (e.g., investment, sustained demand shifts), which could change outcomes. Moreover, we rely on literature-based health damage factors that are indicative and may not fully reflect post-2007 abatement technologies or updated epidemiological evidence. We note these caveats to maintain clarity and transparency in interpreting our results.

6. Robustness

Endogeneity bias: 2SRI versus naive OLS — Column 1 of Appendix Table A4 presents the estimates of a naive OLS regressions that disregards any potential endogeneity bias. The estimated treatment effect of a relative-cost shock, $\mathbb{1}(MC_{\text{gas}} > MC_{\text{coal}})$, is 17,421 in the preferred 2SRI specification versus 16,955 in the naive OLS model – a difference of about 2.7 %. This implies that the endogeneity bias in the naive OLS coefficient is modest in magnitude but still present. The 2SRI specification remains preferable because it explicitly corrects for (weak) gas-price endogeneity and yields a slightly larger point estimate. Hence, corrective 2SRI procedure produces a treatment effect estimate that is close to but somewhat higher than the naive OLS benchmark.

Continuous marginal-cost spread — Our baseline regressor, $\mathbb{1}(MC_{\text{gas}} > MC_{\text{coal}})$, reflects the step-shaped merit order: when gas becomes more expensive than coal, coal units move ahead in the dispatch queue. To assess whether the *magnitude* of this spread matters, we re-estimate the baseline model (Eq. (7)) using the continuous spread $spread = MC_{\text{gas}} - MC_{\text{coal}}$ and its square in a two-stage least squares regression, where we use the Asian gas price and the Australian coal price and their squared terms as instruments. Moreover, we apply decile bins of the spread in a 2SRI regression. The regression outputs are provided in columns 2 and 3 of Appendix Table A4 and the marginal effects of the binned 2SRI regression are visualized in Appendix Fig. A2.

In both regressions, we find positive but *diminishing* marginal effects. In the first regression, the linear term on *spread* is positive and significant (489.6, $p < .01$), while the squared term is negative and significant (-1.33 , $p < .01$), indicating a concave relationship with coal output. The decile-bin regression shows a monotonic increase in predicted coal generation from the lowest to the highest spread, but the increments flatten in the upper bins. Hence, once the marginal-cost ordering flips, larger spreads add relatively little additional coal dispatch. These patterns corroborate the binary-switch specification as an economically meaningful summary of the regime shift.

Adjustment speed — In European electricity markets, unit commitment and dispatch are set in day-ahead (and even intraday) auctions, so coal and gas plants routinely adjust output on a daily – and often hourly – basis. Our dependent variables are daily aggregates of these hourly decisions, and the binary cost-ordering indicator is built from daily marginal costs, mirroring the operational rhythm of the day-ahead market.

However, to allow for slower operational responses (e.g., minimum up/down times, maintenance schedules), we re-estimate the model with lagged switching indicators (lags 1–3 of $\mathbb{1}(MC_{\text{gas}} > MC_{\text{coal}})$) and with a three-day moving average. Across these specifications, coefficients remain qualitatively similar to the baseline (Appendix Fig. A3). None of the lagged or moving-average coefficients is statistically different from the contemporaneous estimate, indicating that our results are not sensitive to assumptions about the exact speed of dispatch adjustment.

Global news/uncertainty — To address the concern that global news shocks may affect EU dispatch outside the price-spread channel, we add the VIX (CBOE) Volatility Index provided by the [Federal Reserve Bank of St. Louis \(2025\)](#) as a daily control, with and without a one-day lag. This index measures market expectation of near term volatility conveyed by stock index option prices. Across both specifications (Appendix Table A5), the switching indicator remains robust and highly significant, while VIX is statistically null individually and in a joint test with its lag. Coefficients on VIX are small in magnitude, indicating limited economic relevance. These results reinforce that our estimates reflect same-day switching on the relative-cost margin rather than a global-news channel.

Timing and expectations — Day-ahead dispatch can reflect both today's relative costs and expectations about tomorrow's costs. We therefore augment the baseline indicator specification by adding an expectations proxy – the *orthogonalized lead* of the instrumented switching indicator, $\hat{1}_{t+1}^\perp$, which we construct as the residual from regressing the lead indicator $\mathbb{1}(MC_{\text{gas}} > MC_{\text{coal}})_{t+1}$ on the contemporaneous indicator ($\mathbb{1}(MC_{\text{gas}} > MC_{\text{coal}})_t$), its lags $t - 1$ and $t - 2$, and the full set of controls. The results (Appendix Table A6, column 1) are intuitive: the expectations proxy is statistically null once today's regime is controlled for, while the contemporaneous indicator keeps the expected sign and remains statistically significant. This check indicates that our main effects are not driven by forward-looking behavior and reflect same-day switching on the relative-cost margin. These results remain qualitatively unchanged when we additionally include a two-day lead, $\mathbb{1}(MC_{\text{gas}} > MC_{\text{coal}})_{t+2}$, as shown in Appendix Table A6, column 2. Both lead terms are statistically insignificant, while the contemporaneous indicator remains statistically significant, has the same sign, and is of similar magnitude.

Moreover, to check short-run persistence, we also include one lag of the switching indicator (Appendix Table A6, column 3). The orthogonalized lead remains statistically null, providing robustness relative to column 1. Both the contemporaneous indicator and its lag are positive and statistically significant (the contemporaneous effect at the 10 % level), so we report the two-day cumulative effect $\mathbb{1}(MC_{\text{gas}} > MC_{\text{coal}})_t + \mathbb{1}(MC_{\text{gas}} > MC_{\text{coal}})_{t-1}$ and a joint test of the two coefficients. The cumulative effect is positive and statistically significant, implying that coal generation rises when coal is relatively cheaper, with the response distributed over yesterday and today. This implies that our baseline regression focusing on the contemporaneous effect is correct in sign and interpretation, but somewhat conservative in magnitude: the baseline contemporaneous estimate is about 17,420 MWh per day when $MC_{\text{gas}} > MC_{\text{coal}}$, whereas the two-day response amounts to about 18,576 MWh per day.

Freight and supply-chain tightness — We augment the second stage with global freight controls to test whether our instruments operate through contemporaneous logistics constraints rather than relative fuel costs. Adding the Baltic Panamax Index (BPI; [investing.com, 2025a](#)) and the Baltic Supramax Index (BSI; [investing.com, 2025b](#)), with and without one lag, leaves the switching indicator large and highly significant across all specifications (Table A7). BPI is never statistically significant; BSI is weakly positive only contemporaneously and becomes insignificant once its lag is included. The estimated coefficients on BPI and BSI (including lags) are

small in magnitude, indicating limited economic relevance. These results indicate that freight-market tightness is not the channel behind our estimates, which continue to reflect same-day switching on the relative-cost margin.

Robustness with switching indicator/price spread and price levels — Table A8 reports five second-stage 2SRI specifications that add fuel price levels to our baseline switching regressions. Columns 1–2 augment the binary switching indicator $1(MC_{gas} > MC_{coal})$ with either P_{gas} or P_{coal} to separate the *switching margin* (relative costs) from *intensive-margin* responses to absolute fuel prices. Conditioning on a single (instrumented) price level shuts down the omitted-variable path from absolute prices to the outcome and isolates the indicator's relative-cost content. If the indicator merely proxied for level effects, its coefficient would collapse toward zero or lose significance once P_{gas} or P_{coal} is included. Instead, the indicator remains positive and statistically significant in both columns, while the added level term is also positive and significant—exactly the pattern consistent with the indicator identifying switching on the *relative-cost* margin and the level capturing *intensive-margin* responses. The significance of $\hat{\epsilon}_{gas}$ and $\hat{\epsilon}_{coal}$ further confirms that price levels are endogenous and validates the 2SRI correction.

Columns 3–4 replace the indicator with the continuous spread ($MC_{gas} - MC_{coal}$) and again include a single price level. Because $MC_{gas} - MC_{coal} = a P_{gas} - b P_{coal}$, the spread coefficient changes sign across the two columns: conditional on P_{gas} it predominantly reflects the coal-cost margin (negative), whereas conditional on P_{coal} it reflects the gas-cost margin (positive). In both cases the level term is positive and significant,

Column 5 includes both P_{gas} and P_{coal} (together with $\hat{\epsilon}_{gas}$, $\hat{\epsilon}_{coal}$) without the indicator or spread. The positive coefficient on P_{coal} should *not* be read as “a higher coal price causes more coal generation.” It is a *partial* effect conditional on P_{gas} in a context where fuel prices co-move strongly; the economically meaningful margin is the *relative cost*. To map column 5 to that relative-cost margin, note that our marginal costs scale prices by inverse electric efficiencies (see Eq. (1)): for a one-unit change in the fuel price, $a \equiv \partial MC_{gas}/\partial P_{gas} = 1/\rho_{gas}$ and $b \equiv \partial MC_{coal}/\partial P_{coal} = 1/\rho_{coal}$ (with the same unit conversions used in constructing MC). Hence, $S \equiv MC_{gas} - MC_{coal} = a P_{gas} - b P_{coal}$ and the implied spread effect from the levels-only regression is $\beta_S = a \hat{\beta}_{P_{gas}} - b \hat{\beta}_{P_{coal}}$. Using the same (a, b) as in our marginal-cost construction (i.e., $a = 1/\rho_{gas}$ and $b = 1/\rho_{coal}$), β_S has the same sign and order of magnitude as in columns 3–4 and in the indicator specifications: when gas becomes relatively more expensive than coal (the spread widens), coal generation increases. Thus, the levels-only specification is consistent with the switching interpretation; the positive $\hat{\beta}_{P_{coal}}$ is a conditional partial effect, not a structural own-price elasticity.

Across all columns, the sign and magnitude on the relative-cost margin are stable and show that making gas relatively more expensive increases coal generation; adding instrumented price levels alongside the indicator or spread leaves this core switching result intact while confirming that absolute price levels matter on the intensive margin.

7. Conclusion

Europe's 2021/22 gas price surge, triggered by geopolitical events, reordered relative marginal costs between gas and coal and, in turn, altered electricity dispatch. While right before the crisis, a high price for EU CO₂ allowances ensured that electricity production from gas was cheaper than that of coal, the shock to relative fuel prices led to a gas-to-coal fuel switch. Our study focuses on the environmental and health implications of this relative-cost shock: when $MC_{gas} > MC_{coal}$, coal moves ahead of gas in the merit order and is dispatched more intensively.

Using a causal 2SRI design on daily data (2015–2023) for six EU countries with substantial gas-to-coal switching potential, and instrumenting European fuel prices with exogenous benchmarks from other regions, we isolate the effect of the marginal-cost reversal on coal-fired generation, CO₂, local air pollutants, and indicative health outcomes. We estimate that coal-fired electricity rose by 23 % (53 TWh; 95 % CI: 43–63 TWh), CO₂ emissions by 10 % (36 MtCO₂; 95 % CI: 28–45 Mt), PM_{2.5} by 19 % (187 t, 95 % CI: 152–222 t), NO_x by 10 % (8,442 t, 95 % CI: 6,573–10,715 t), and SO₂ by 24 % (16,238 t, 95 % CI: 10,947–21,658 t). Applying literature-based damage factors, we obtain illustrative estimates that premature deaths and serious illnesses rose significantly (by 17 %), implying external health costs exceeding one billion EUR₂₀₂₁. These health figures should be interpreted strictly as indicative orders of magnitude, not causal health estimates, because they rely on static literature values that may not reflect post-2007 abatement technologies or updated epidemiology.

Our results demonstrate that ensuring supply adequacy through additional coal dispatch in response to fuel price shocks carries substantial environmental and health costs. They also yield several policy-relevant insights. First, the implied “no-switch” carbon price peaks around 760 €/tCO₂ (average 198 €/tCO₂ versus an observed 75 €/tCO₂), underscoring that even well-functioning carbon markets can be stressed by extreme shocks. Second, fixed emission caps (and the resulting “waterbed effect”) and other market-based instruments may be vulnerable to sudden relative-price shifts, suggesting the need for stabilizing mechanisms or complementary measures. Third, our results demonstrate that effective crisis management may require a balanced portfolio of instruments: market-based tools to preserve efficiency and provide long-run signals, complemented by temporary command-and-control measures, such as dispatch constraints and targeted subsidies, to contain short-term externalities.

Finally, while it is beyond our empirical scope to model clean-energy deployment, our findings imply that reducing exposure to volatile fossil-fuel price spreads can lower the risk of environmentally costly switching episodes. We therefore frame investments in low-emission generation and demand-side flexibility as policy implications, not direct empirical results. Any comprehensive cost-benefit assessment should weigh these potential long-run benefits against the short-run external costs we quantify here.

Declaration of generative AI and AI-assisted technologies in the writing process

During the preparation of this work the authors used ChatGPT in order to improve the language and style of the text. After using this tool, the authors reviewed and edited the content as needed and take full responsibility for the content of the published article.

Disclosure statement

We hereby declare that we have no conflicts of interest or financial disclosures to report related to this manuscript.

Data availability

The data and models used in this study were processed in Stata 18 and are available on GitHub at <https://github.com/mliebens/From-Gas-to-Coal>.

Declaration of competing interest

The authors declare no competing interests.

Appendix A. Appendix

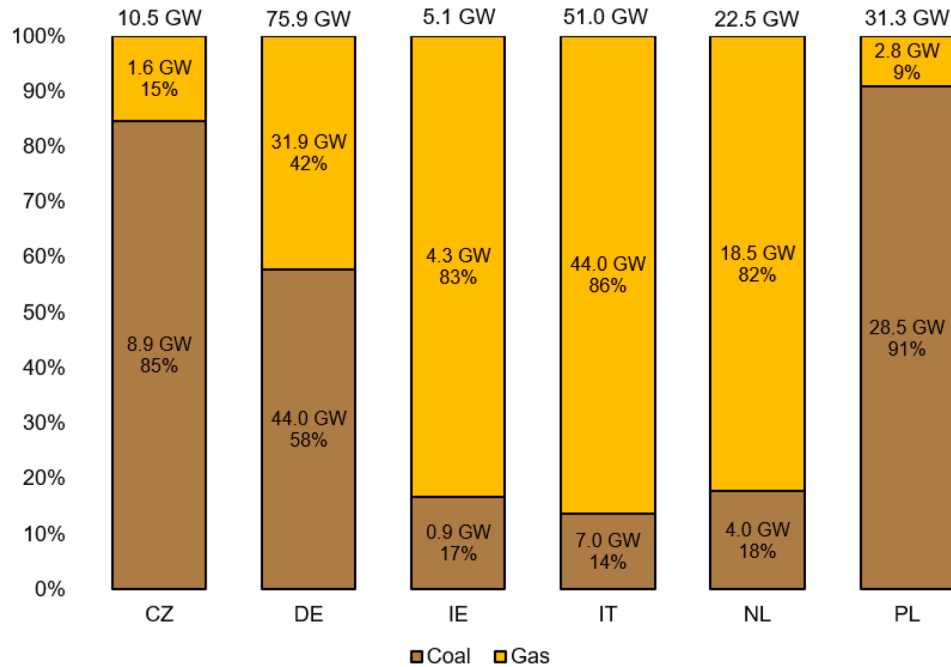


Fig. A1. Share of coal and gas capacity. This figure depicts the 2021 capacity shares of coal and gas the six sample countries. “Coal” encompasses both hard coal and lignite. Data source: ENTSO-E (2024).

Table A1

Efficiency factors by ture vintage, ture type, and fuel type.

Fuel type	Turb type	Vintage (online until)	Efficiency factor (ρ)	Fuel type	Turb type	Vintage (online until)	Efficiency factor (ρ)
LI	ST	1955	0.29	HC	ST	2000	0.45
LI	ST	1960	0.3	HC	ST	2023	0.48
LI	ST	1965	0.31	NG	GT	1970	0.3
LI	ST	1970	0.32	NG	GT	1980	0.33
LI	ST	1975	0.33	NG	GT	1990	0.35
LI	ST	1980	0.35	NG	GT	2024	0.38
LI	ST	1985	0.37	NG	ST	1950	0.3
LI	ST	1990	0.39	NG	ST	1960	0.34
LI	ST	1995	0.42	NG	ST	1970	0.36
LI	ST	2000	0.44	NG	ST	1980	0.38
LI	ST	2005	0.45	NG	ST	1990	0.42
LI	ST	2023	0.47	NG	ST	2023	0.44
HC	ST	1955	0.3	NG	CC	1980	0.44
HC	ST	1960	0.31	NG	CC	1985	0.47
HC	ST	1965	0.32	NG	CC	1990	0.52
HC	ST	1970	0.33	NG	CC	1995	0.56
HC	ST	1975	0.34	NG	CC	2000	0.59
HC	ST	1980	0.36	NG	CC	2005	0.6
HC	ST	1985	0.38	NG	CC	2014	0.61
HC	ST	1990	0.4	NG	IC	1980	0.34
HC	ST	1995	0.43	NG	IC	2014	0.35

Notes: LI = lignite, HC = hard coal, NG = natural gas, ST = steam ture, GT = gas ture, CC = comed cycle, IC = internal combustion.

Table A2

Capacity-weighted efficiency factors applied in our sample.

Country	Year	ρ_{NG}	ρ_{HC}	ρ_{LI}	Country	Year	ρ_{NG}	ρ_{HC}	ρ_{LI}
CZ	2015	0.551	0.394	0.360	IT	2015	0.582	0.429	0.320
CZ	2016	0.551	0.394	0.360	IT	2016	0.582	0.429	0.320
CZ	2017	0.551	0.394	0.368	IT	2017	0.582	0.429	0.320
CZ	2018	0.551	0.394	0.370	IT	2018	0.582	0.431	0.320
CZ	2019	0.551	0.394	0.370	IT	2019	0.582	0.431	0.320
CZ	2020	0.551	0.394	0.384	IT	2020	0.583	0.434	0.320
CZ	2021	0.551	0.394	0.390	IT	2021	0.583	0.434	0.320
CZ	2022	0.551	0.394	0.390	IT	2022	0.583	0.434	0.320
CZ	2023	0.551	0.394	0.390	IT	2023	0.583	0.434	0.320
CZ	2024	0.551	0.394	0.390	IT	2024	0.583	0.434	0.320
DE	2015	0.503	0.401	0.390	NL	2015	0.547	0.437	NA
DE	2016	0.511	0.404	0.390	NL	2016	0.543	0.455	NA
DE	2017	0.512	0.405	0.390	NL	2017	0.542	0.455	NA
DE	2018	0.514	0.412	0.390	NL	2018	0.541	0.467	NA
DE	2019	0.514	0.413	0.394	NL	2019	0.539	0.467	NA
DE	2020	0.514	0.415	0.394	NL	2020	0.537	0.467	NA
DE	2021	0.516	0.415	0.394	NL	2021	0.537	0.467	NA
DE	2022	0.506	0.416	0.397	NL	2022	0.537	0.467	NA
DE	2023	0.524	0.419	0.402	NL	2023	0.544	0.467	NA
DE	2024	0.529	0.419	0.408	NL	2024	0.544	0.467	NA
IE	2015	0.544	0.415	NA	PL	2015	0.592	0.370	0.366
IE	2016	0.544	0.415	NA	PL	2016	0.592	0.372	0.366
IE	2017	0.544	0.415	NA	PL	2017	0.585	0.378	0.366
IE	2018	0.544	0.415	NA	PL	2018	0.592	0.379	0.370
IE	2019	0.544	0.415	NA	PL	2019	0.589	0.396	0.370
IE	2020	0.544	0.415	NA	PL	2020	0.587	0.400	0.375
IE	2021	0.541	0.415	NA	PL	2021	0.587	0.401	0.375
IE	2022	0.531	0.415	NA	PL	2022	0.588	0.404	0.375
IE	2023	0.546	0.415	NA	PL	2023	0.588	0.410	0.375
IE	2024	0.566	0.415	NA	PL	2024	0.588	0.410	0.375

Notes: LI = lignite, HC = hard coal, NG = natural gas, NA = not available, meaning that the country has no such power plants. If an efficiency factor does not vary over the years, it means that no new power plants in this fuel category have come online during that time.

Table A3
Deaths per TWh by fuel.

Fuel	Change in production (TWh) (JDJ22, Tab. 2)	Change in mortality (# deaths) (JDJ22, Tab. 4)	Deaths per TWh in Germany (JDJ22)	Deaths per TWh in Europe (MW07)
Lignite	188.5	7.6	24.8	32.6
Hard coal	542.7	16.7	32.5	24.5
Natural gas	38.6	4.9	7.9	2.8

JDJ22 ... Jarvis et al. (2022), MW07 ... Markandya and Wilkinson (2007). Markandya and Wilkinson (2007) report Europe-wide mortality factors by technology, whereas Jarvis et al. (2022) provide estimates for Germany based on the nuclear phase-out.

Table A4
Robustness: continuous cost spread & adjustment speed.

	(1)	(2)	(3)
	OLS	2SLS	2SRI
	Coal gen.	Coal gen.	Coal gen.
$\mathbb{1}(MC_{gas} > MC_{coal})$	16955.0*** (1646.8)		
Spread		489.6*** (34.95)	
Spread ²		-1.325*** (0.140)	
$\hat{\epsilon}_{gas}$			42.55 (40.91)
$\hat{\epsilon}_{coal}$			-215.0 (177.7)
Baseload	-0.0362 (0.0272)	-0.0363 (0.0270)	-0.0389 (0.0269)
Load	0.427*** (0.00920)	0.425*** (0.00915)	0.424*** (0.00909)
VRE	-0.461*** (0.00686)	-0.458*** (0.00679)	-0.459*** (0.00674)
Bin2			4119.7** (1932.1)
Bin3			15138.0*** (2029.7)
Bin4			23821.0*** (2050.0)
Bin5			25066.1*** (2813.2)
Bin6			28543.1*** (2872.8)
Bin7			29390.9*** (2798.0)
Bin8			35075.4*** (2721.0)
Bin9			30175.5*** (2705.7)
Bin10			40644.0*** (2675.3)
Country×Year FE	yes	yes	yes
Month FE	yes	yes	yes
Day-of-week FE	yes	yes	yes
Observations	19,322	19,322	19,322
R-squared	0.955	0.955	0.956
K.P. first-stage F		576	504

Notes: Column 1 reports the naive OLS specification with the binary switching indicator. Column 2 instruments the continuous marginal-cost spread ($MC_{gas} - MC_{coal}$) and its square with Asian gas and Australian coal prices (and their squares) in a 2SLS regression. Column 3 uses decile bins of the continuous marginal-cost spread in a 2SRI regression. $\hat{\epsilon}_{coal,i,t}$ and $\hat{\epsilon}_{gas,i,t}$ are the fitted residuals from the first-stage regressions. "K.P." denotes the Kleibergen-Paap rk Wald F statistic. HAC (Newey-West, bw = 2) standard errors in parentheses. Significance: * $p < 0.10$, ** $p < 0.05$, *** $p < 0.01$.

Table A5
Robustness: global-news control (VIX).

	(1)	(2)
2SRI	2SRI	
Coal gen.	Coal gen.	
Indicator + VIX	Indicator + VIX + lag	
$\mathbb{1}(MC_{gas} > MC_{coal})$	17337.04*** (1673.26)	17336.77*** (1673.29)
VIX _t	71.92 (64.95)	214.54 (154.93)
VIX _{t-1}		-149.47 (155.42)
$\hat{\epsilon}_{gas}$	73.33* (39.98)	73.17* (39.97)
$\hat{\epsilon}_{coal}$	-226.27 (176.22)	-223.37 (176.23)
Baseload	-0.0362 (0.0272)	-0.0356 (0.0272)
Load	0.427*** (0.00920)	0.427*** (0.00921)
VRE	-0.462*** (0.00685)	-0.461*** (0.00686)
Observations	19,322	19,318
R-squared	0.955	0.955
Country \times Year FE	Yes	Yes
Month FE	Yes	Yes
Day-of-week FE	Yes	Yes

Notes: All specifications include the control-function residuals ($\hat{\epsilon}_{gas}, \hat{\epsilon}_{coal}$), country \times year, month, and day-of-week fixed effects. HAC (Newey-West, bw = 2) standard errors in parentheses. Significance: * p < 0.10, ** p < 0.05, *** p < 0.01.

Table A6
Robustness: timing and expectations.

	(1)	(2)	(3)
2SRI	2SRI	2SRI	
Coal gen.	Coal gen.	Coal gen.	
Indicator +	Indicator +	Indicator +	
expect. proxy	2 expect. proxies	expect. proxy + lag	
$\mathbb{1}(MC_{gas} > MC_{coal})_t$	17404.2*** (1674.6)	17404.5*** (1673.2)	6063.5* (3561.2)
$\hat{\mathbb{1}}^{\perp}_{-t+1}$	4310.7 (3021.8)	3388.8 (4064.1)	4299.0 (3004.9)
$\hat{\mathbb{1}}^{\perp}_{-t+2}$		1298.0 (4476.0)	
$\mathbb{1}(MC_{gas} > MC_{coal})_{t-1}$			12512.2*** (3614.2)
$\hat{\epsilon}_{gas}$	78.65** (39.89)	79.22** (39.87)	85.69** (39.82)
$\hat{\epsilon}_{coal}$	-224.1 (176.1)	-223.9 (176.2)	-217.3 (175.8)
Baseload	-0.0356 (0.0272)	-0.0355 (0.0272)	-0.0359 (0.0272)
Load	0.426*** (0.00921)	0.426*** (0.00922)	0.426*** (0.00921)
VRE	-0.461*** (0.00686)	-0.461*** (0.00686)	-0.461*** (0.00685)
Country \times Year FE	yes	yes	yes
Month FE	yes	yes	yes
Day-of-week FE	yes	yes	yes
Observations	19,307	19,302	19,307
R-squared	0.955	0.955	0.955
Cumulat. effect $\mathbb{1}_t + \mathbb{1}_{t-1}$			18,575.8
Cumulative S.E.			1,726.9
Cumulative p-value			0.000
Joint p-value			0.000

Notes: The expectations proxies are orthogonalized leads of the instrumented switching indicator, $\hat{\mathbb{1}}^{\perp}_{-t+1}, \hat{\mathbb{1}}^{\perp}_{-t+2}, \hat{\epsilon}_{coal;i,t}$ and $\hat{\epsilon}_{gas;i,t}$ are the fitted residuals from the first-stage regressions. HAC (Newey-West, bw = 2) standard errors in parentheses. Significance: * p < 0.10, ** p < 0.05, *** p < 0.01.

Table A7

Robustness: Baltic Panamax (BPI) and Baltic Supramax (BSI).

	(1)	(2)	(3)	(4)
2SRI	2SRI	2SRI	2SRI	2SRI
Coal gen.	Coal gen.	Coal gen.	Coal gen.	Coal gen.
BPI	BPI + lag	BSI	BSI	BSI + lag
$\mathbb{1}(MC_{gas} > MC_{coal})$	17298.43*** (1704.09)	17377.41*** (1716.70)	16044.61*** (1797.21)	16184.37*** (1807.69)
BPI _t	0.565 (1.086)	7.673 (8.728)		
BPI _{t-1}		-7.126 (8.724)		
BSI _t			3.733** (1.472)	22.982 (18.960)
BSI _{t-1}				-19.250 (18.918)
$\hat{\epsilon}_{gas}$	86.58** (43.93)	85.61* (43.91)	125.31*** (43.94)	123.83*** (44.03)
$\hat{\epsilon}_{coal}$	-281.23 (198.22)	-276.99 (198.22)	-586.14*** (222.15)	-587.53*** (222.20)
Baseload	-0.0359 (0.0272)	-0.0353 (0.0272)	-0.0346 (0.0271)	-0.0340 (0.0271)
Load	0.427*** (0.00918)	0.426*** (0.00919)	0.426*** (0.00917)	0.426*** (0.00918)
VRE	-0.462*** (0.00685)	-0.461*** (0.00686)	-0.462*** (0.00685)	-0.462*** (0.00685)
Country × Year FE	Yes	Yes	Yes	Yes
Month FE	Yes	Yes	Yes	Yes
Day-of-week FE	Yes	Yes	Yes	Yes
Observations	19,322	19,318	19,322	19,318
R-squared	0.955	0.955	0.955	0.955
p-value: $H_0 : BPI_t + BPI_{t-1} = 0$		0.6152		0.0112
p-value: $H_0 : BSI_t + BSI_{t-1} = 0$				

Notes: ($\hat{\epsilon}_{gas}$, $\hat{\epsilon}_{coal}$) are control-function residuals from the first stage. Columns 1–2 add the Baltic Panamax Index (BPI) contemporaneously and with one lag; columns 3–4 add the Baltic Supramax Index (BSI) contemporaneously and with one lag. $\hat{\epsilon}_{gas;i,t}$ and $\hat{\epsilon}_{coal;i,t}$ are the fitted residuals from the first-stage regressions. HAC (Newey–West, bw = 2) standard errors in parentheses. Significance: * $p < .10$, ** $p < .05$, *** $p < .01$.

Table A8

Robustness regressions including gas and coal price levels.

	(1)	(2)	(3)	(4)	(5)
	2SRI	2SRI	2SRI	2SRI	2SRI
Coal gen.	Coal gen.	Coal gen.	Coal gen.	Coal gen.	Coal gen.
Indicator + P _{gas}	Indicator + P _{coal}	Spread + P _{gas}	Spread + P _{coal}	P _{gas} + P _{coal}	
	(1)	(2)	(3)	(4)	(5)
$\mathbb{1}(MC_{gas} > MC_{coal})$	5472.2*** (1956.7)	6957.0*** (1866.5)			
Spread			-284.4*** (81.79)	102.5*** (24.20)	
P _{gas}	273.8*** (24.01)		694.0*** (112.9)		197.8*** (40.58)
P _{coal}		1559.3*** (143.4)		1157.8*** (209.5)	790.3*** (254.4)
$\hat{\epsilon}_{gas}$	-267.1*** (51.87)	12.51 (40.25)	-196.5*** (58.55)	-214.2*** (57.74)	-223.3*** (54.72)
$\hat{\epsilon}_{coal}$	-301.2* (174.6)	-1872.2*** (240.5)	-1046.4*** (282.0)	-1235.7*** (335.4)	-1124.6*** (331.0)
Baseload	-0.0330 (0.0270)	-0.0324 (0.0271)	-0.0303 (0.0271)	-0.0327 (0.0271)	-0.0320 (0.0271)
Load	0.427*** (0.00915)	0.427*** (0.00915)	0.427*** (0.00915)	0.428*** (0.00914)	0.427*** (0.00915)
VRE	-0.458*** (0.00681)	-0.459*** (0.00677)	-0.458*** (0.00681)	-0.458*** (0.00680)	-0.458*** (0.00679)
Country × Year FE	Yes	Yes	Yes	Yes	Yes
Month FE	Yes	Yes	Yes	Yes	Yes
Day-of-week FE	Yes	Yes	Yes	Yes	Yes
Observations	19,322	19,322	19,322	19,322	19,322
R-squared	0.955	0.955	0.955	0.955	0.955

Notes: Columns 1 & 2 add the prices of gas and coal, respectively, to the binary switching indicator $\mathbb{1}(MC_{gas} > MC_{coal})$. Columns 3 & 4 include the prices of gas and coal, respectively, alongside the continuous spread ($MC_{gas} - MC_{coal}$). Column 5 employs the prices of gas and hard coal instead of the binary indicator. $\hat{\epsilon}_{gas;i,t}$ and $\hat{\epsilon}_{coal;i,t}$ are the fitted residuals from the first-stage regressions. HAC (Newey-West, bw = 2) standard errors in parentheses. Significance: * $p < 0.10$, ** $p < 0.05$, *** $p < 0.01$.

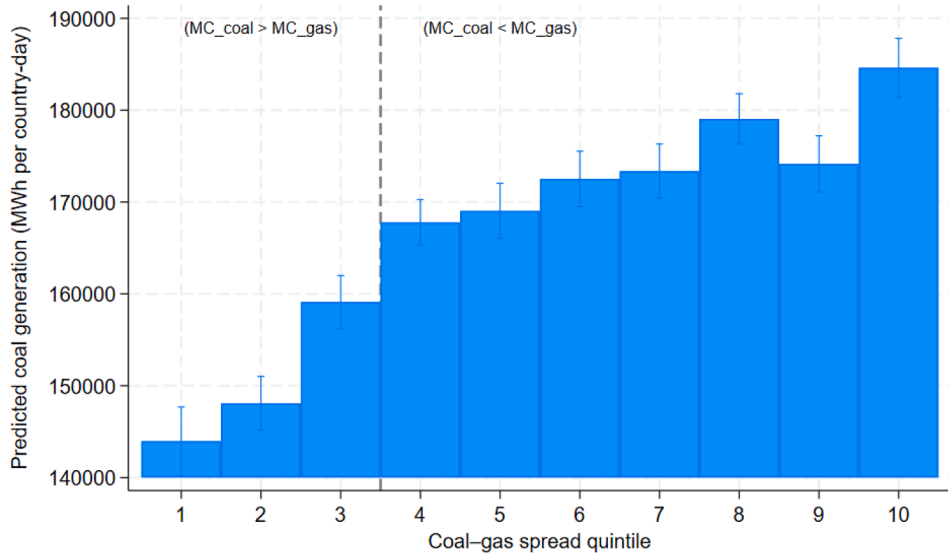


Fig. A2. Predicted coal generation per coal-gas spread quintile bin. Note that coal generation remains positive even in bins with $MC_{coal} > MC_{gas}$ because some units operate at technical minimum (“must-run”) and coal may still be required to meet demand once gas and other technologies are exhausted.

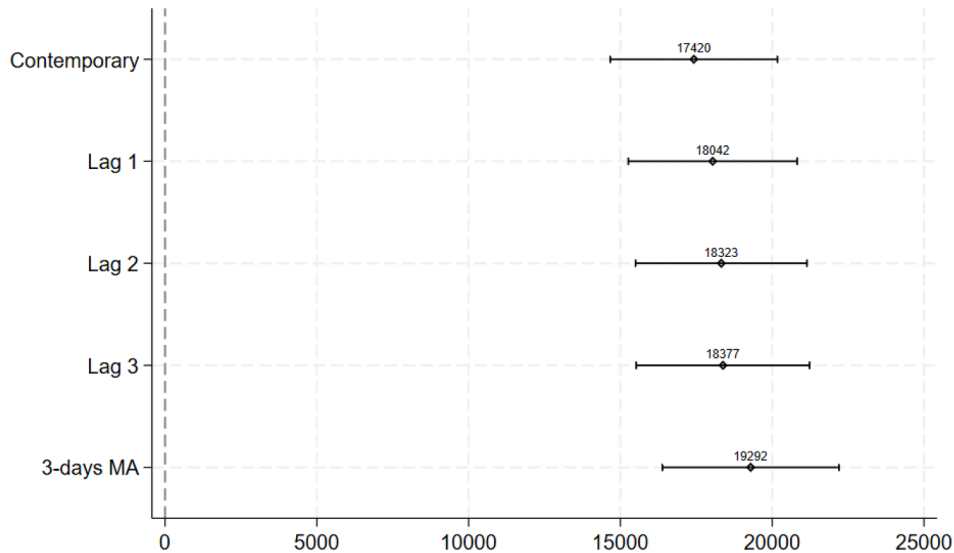


Fig. A3. Speed of adjustment. Notes: This Figure plots coefficient estimates and their 95 % CI for the lagged switching indicators $\mathbb{1}(MC_{gas} > MC_{coal})_{t-1}$, $\mathbb{1}(MC_{gas} > MC_{coal})_{t-2}$, $\mathbb{1}(MC_{gas} > MC_{coal})_{t-3}$, and a three-day moving average. Estimates come from separate 2SRI second-stage regressions with HAC (Bartlett, $bw = 2$) standard errors and the full set of controls and fixed effects.

References

Barreira, A., Patierno, M., Bautista, C.R., 2017. Impacts of pollution on our health and the planet: the case of coal power plants. *Perspect* 28, 1–10.

Bondy, M., Roth, S., Sager, L., 2020. Crime is in the air: the contemporaneous relationship between air pollution and crime. *J. Assoc. Environ. Resour. Econom.* 7 (3), 555–585.

Burt, E., Orris, P., Buchanan, S., 2013. Scientific Evidence of Health Effects from Coal use in Energy Generation. Chicago and Washington: School of Public Health, University of Illinois and Health Care Without Harm.

Carneiro, J., Cole, M.A., Strobl, E., 2021. The effects of air pollution on students' cognitive performance: evidence from Brazilian university entrance tests. *J. Assoc. Environ. Resour. Econom.* 8 (6), 1051–1077.

Carugno, M., Consonni, D., Randi, G., Catelan, D., Grisotto, L., Bertazzi, P.A., Biggeri, A., Baccini, M., 2016. Air pollution exposure, cause-specific deaths and hospitalizations in a highly polluted Italian region. *Environ. Res.* 147, 415–424.

Chang, T.Y., Graff Zivin, J., Gross, T., Neidell, M., 2019. The effect of pollution on worker productivity: evidence from call center workers in China. *Am. Econ. J. Appl. Econom.* 11 (1), 151–172.

Chay, K.Y., Greenstone, M., 2003. The impact of air pollution on infant mortality: evidence from geographic variation in pollution shocks induced by a recession. *Q. J. Econ.* 118 (3), 1121–1167.

Colgan, J.D., Gard-Murray, A.S., Hinthon, M., 2023. Quantifying the value of energy security: how Russia's invasion of Ukraine exploded Europe's fossil fuel costs. *Energy Res. Soc. Sci.* 103, 103201.

Cruz, E., D'alelio, S.J., Stolzenberg, L., 2022. Air pollution and violent criminal behaviour. *Br. J. Criminol.* 62 (2), 450–467.

Cullen, J., 2013. Measuring the environmental benefits of wind-generated electricity. *Am. Econ. J. Econ. Policy* 5 (4), 107–133.

Cullen, J.A., Mansur, E.T., 2017. Inferring carbon abatement costs in electricity markets: a revealed preference approach using the shale revolution. *Am. Econ. J. Econ. Policy* 9 (3), 106–133.

Deschenes, O., Greenstone, M., Shapiro, J.S., 2017. Defensive investments and the demand for air quality: evidence from the NOx budget program. *Am. Econ. Rev.* 107 (10), 2958–2989.

Duque, V., Gilraine, M., 2022. Coal use, air pollution, and student performance. *J. Public Econ.* 213, 104712.

EC, 2023. State aid: Commission approves prolonged and amended Spanish and Portuguese measure to lower electricity prices amid energy crisis. European Commission, Press release, October 25, https://ec.europa.eu/commission/presscorner/detail/en/ip_23_2408.

EEA, 2020. Air Quality in Europe: 2020 Report. European Environment Agency, <https://www.eea.europa.eu/publications/air-quality-in-europe-2020-report>.

EEA, 2024. Estimating the External Costs of Industrial Air Pollution: Trends 2012–2021. Technical Note on the Methodology and Additional Results from the EEA Briefing 24/2023. European Environmental Agency, <https://www.eea.europa.eu/publications/the-cost-to-health-and-the/technical-note-estimating-the-external-costs/view>.

EMBER, 2024. Soaring fossil gas costs responsible for EU electricity price increase. <https://ember-energy.org/latest-insights/soaring-fossil-gas-costs-responsible-for-eu-electricity-price-increase>, accessed on October 28, 2024.

ENTSO-E, 2024. Transparency platform. <https://transparency.entsoe.eu/>, accessed on January 24, 2024.

Eurostat, 2024. Energy balances (database code: nrg_bal_s). https://ec.europa.eu/eurostat/databrowser/view/nrg_bal_s/default/table. Dataset accessed 17 July 2025.

Federal Reserve Bank of St. Louis, 2025. CBOE Volatility Index (VIX) [VIXCLS]. <https://fred.stlouisfed.org/series/VIXCLS>, accessed on October 10, 2025.

Fell, H., Kaffine, D.T., 2018. The fall of coal: joint impacts of fuel prices and renewables on generation and emissions. *Am. Econ. J. Econ. Policy* 10 (2), 90–116.

Geng, G., Zheng, Y., Zhang, Q., Xue, T., Zhao, H., Tong, D., Zheng, B., Li, M., Liu, F., Hong, C., et al., 2021. Drivers of PM2.5 air pollution deaths in China 2002–2017. *Nat. Geosci.* 14 (9), 645–650.

Gillingham, K., Stock, J.H., 2018. The cost of reducing greenhouse gas emissions. *J. Econ. Perspect.* 32 (4), 53–72.

Gugler, K., Haxhimusa, A., Liebensteiner, M., 2021. Effectiveness of climate policies: carbon pricing vs. subsidizing renewables. *J. Environ. Econ. Manage.* 106, 102405.

Gugler, K., Haxhimusa, A., Liebensteiner, M., 2023. Carbon pricing and emissions: causal effects of Britain's carbon tax. *Energy Econ.* 121, 106655.

Gugler, K., Haxhimusa, A., Liebensteiner, M., Schindler, N., 2020. Investment opportunities, uncertainty, and renewables in European electricity markets. *Energy Econ.* 85, 104575.

Hendryx, M., Zullig, K.J., Luo, J., 2020. Impacts of coal use on health. *Annu. Rev. Public Health* 41, 397–415.

Henneman, L., et al., 2023. Mortality risk from United States coal electricity generation. *Science* 382 (6673), 941–946.

Herrnstadt, E., Heyes, A., Muehlegger, E., Saberian, S., 2021. Air pollution and criminal activity: microgeographic evidence from Chicago. *Am. Econ. J. Appl. Econ.* 13 (4), 70–100.

Herweg, F., Schmidt, K.M., 2022. How to regulate carbon emissions with climate-conscious consumers. *Econ. J.* 132 (648), 2992–3019.

Hirth, L., Khanna, T.M., Ruhnau, O., 2024. How aggregate electricity demand responds to hourly wholesale price fluctuations. *Energy Econ.* 135, 107652.

Holladay, J.S., LaRiviere, J., 2017. The impact of cheap natural gas on marginal emissions from electricity generation and implications for energy policy. *J. Environ. Econ. Manage.* 85, 205–227.

Holland, S.P., Mansur, E.T., Muller, N.Z., Yates, A.J., 2020. Decompositions and policy consequences of an extraordinary decline in air pollution from electricity generation. *Am. Econ. J. Econ. Policy* 12 (4), 244–274.

Honscha, L.C., Penteado, J.O., de Sá Gama, V., da Silva Bonifácio, A., Aikawa, P., Dos Santos, M., Baisch, P. R.M., Muccillo-Baisch, A.L., da Silva Júnior, F. M.R., 2021. Health impact assessment of air pollution in an area of the largest coal mine in Brazil. *Environ. Sci. Pollut. Res.*, 1–9.

ICAP, 2024. EU ETS Market Stability Reserve (msr) – Factsheet. International Carbon Action Partnership, <https://icapcarbonaction.com/en/ets/eu-ets-market-stability-reserve-msr>.

investing.com, 2024a. Carbon emissions futures. <https://www.investing.com/commodities/carbon-emissions>, accessed on January 24, 2024.

investing.com, 2024b. Coal (API2) CIF ARA (ARGUS-McCloskey) Futures (MTFc1). <https://www.investing.com/commodities/ice-dutch-ttf-gas-c1-futures>, accessed on January 24, 2024.

investing.com, 2024c. ICE Dutch TTF natural gas futures. <https://www.investing.com/commodities/ice-dutch-ttf-gas-c1-futures>, accessed on January 24, 2024.

investing.com, 2024d. LNG Japan/Korea marker PLATTS future (JKMc1). <https://www.investing.com/commodities/lnj-japan-korea-marker-platts-futures>, accessed on July 19, 2025.

investing.com, 2024e. Newcastle Coal (NCFMc1). <https://www.investing.com/commodities/newcastle-coal-futures>, accessed on July 19, 2025.

investing.com, 2025a. Baltic Panamax (BPI). <https://www.investing.com/indices/baltic-panamax-historical-data>, accessed on October 10, 2025.

investing.com, 2025b. Baltic Supramax (BSIS). <https://www.investing.com/indices/baltic-supramax-historical-data>, accessed on October 10, 2025.

IPCC, 2006. Chapter 2: stationary combustion. Intergovernmental Panel on Climate Change, https://www.ipcc-nccip.iges.or.jp/public/2006gl/pdf/2_Volume2/V2_2_Ch2_Stationary_Combustion.pdf.

Jarvis, S., Deschenes, O., Jha, A., 2022. The private and external costs of Germany's nuclear phase-out. *J. Eur. Econ. Assoc.* 20 (3), 1311–1346.

Jerrett, M., 2015. The death toll from air-pollution sources. *Nature* 525 (7569), 330–331.

Knittel, C.R., Metaxoglou, K., Trindade, A., 2019. Environmental implications of market structure: shale gas and electricity markets. *Int. J. Ind. Organiz.* 63, 511–550.

Kotek, P., Selei, A., Tóth, B.T., Felsmann, B., 2023. What can the EU do to address the high natural gas prices? *Energy Policy* 173, 113312.

Lichter, A., Pestel, N., Sommer, E., 2017. Productivity effects of air pollution: evidence from professional soccer. *Labour Econ.* 48, 54–66.

Markandya, A., Wilkinson, P., 2007. Electricity generation and health. *The Lancet* 370 (9591), 979–990.

McCarron, A., Semple, S., Braban, C.F., Gillespie, C., Swanson, V., Price, H.D., 2023. Personal exposure to fine particulate matter (PM2.5) and self-reported asthma-related health. *Soc. Sci. Med.* 337, 116293.

Milov, V., 2022. European gas price crisis: is Gazprom responsible? *Eur. View* 21 (1), 66–73.

Moore, E., Chatzidiakou, L., Kuku, M.-O., Jones, R.L., Smeeth, L., Beevers, S., Kelly, F.J., Barratt, B., Quint, J.K., 2016. Global associations between air pollutants and chronic obstructive pulmonary disease hospitalizations: a systematic review. *Ann. Am. Thorac. Soc.* 13 (10), 1814–1827.

Perino, G., 2018. New EU ETS phase 4 rules temporarily puncture the waterbed. *Nat. Clim. Chang.* 8 (4), 262–264.

Petrowski, K., Bührer, S., Strauß, B., Decker, O., Brähler, E., 2021. Examining air pollution (PM10), mental health and well-being in a representative German sample. *Sci. Rep.* 11 (1), 18436.

Quaschning, V., 2024. Specific carbon dioxide emissions of various fuels. <https://www.volker-quaschning.de/datserv/CO2-spez>, accessed on January 24, 2024.

Ren, T., Yu, X., Yang, W., 2019. Do cognitive and non-cognitive abilities mediate the relationship between air pollution exposure and mental health? *PLoS ONE* 14 (10), e0223353.

Rennert, K., et al., 2022. Comprehensive evidence implies a higher social cost of CO2. *Nature* 610 (7933), 687–692.

Ritchie, H., 2020. What are the safest and cleanest sources of energy? Our World in Data, <https://ourworldindata.org/safest-sources-of-energy>.

Rosendahl, K.E., 2019. EU ETS and the waterbed effect. *Nat. Clim. Chang.* 9 (10), 734–735.

Ruhnau, O., Stiewe, C., Muessel, J., Hirth, L., 2023. Natural gas savings in Germany during the 2022 energy crisis. *Nat. Energy* 8 (6), 621–628.

S&P Global, 2024. Platts powervision power plant database. <https://www.spglobal.com/commodityinsights/en/products-services/electric-power/powervision>, access on July 21, 2024.

Terza, J.V., Basu, A., Rathouz, P.J., 2008. Two-stage residual inclusion estimation: addressing endogeneity in health econometric modeling. *J. Health Econ.* 27 (3), 531–543.

UBA, 2019. Updating the Emission Factors for Large Combustion Plants. German Environment Agency (Umweltbundesamt, UBA).

UBA, 2022. CO2 Emission Factors for Fossil Fuels: Update 2022. German Environment Agency (Umweltbundesamt, UBA).

UBA, 2022. Review of the EU ETS Market Stability Reserve (msr): Options for Strengthening and Prolonging the Instrument. German Environment Agency (Umweltbundesamt), <https://www.umweltbundesamt.de/publikationen/review-of-the-eu-ets-market-stability-reserve-msr>.

Wang, Y., Zhang, Z., Hao, Z., Eriksson, T., 2025. Environmental regulation and mental well-being: evidence from China's air pollution prevention and control action plan. *Soc. Sci. Med.* 365, 117584.

Weitzel, M., Vandyck, T., Garaffa, R., Temursho, U., Ordonez, J.A., Tamba, M., 2024. The effects of higher gas prices on the EU economy: a computable general equilibrium modelling perspective. *Environ. Res. Energy* 1 (3), 035006.

Wilson, I.A.G., Staffell, I., 2018. Rapid fuel switching from coal to natural gas through effective carbon pricing. *Nat. Energy* 3 (5), 365–372.

Wooldridge, J.M., 2015. Control function methods in applied econometrics. *J. Human Resour.* 50 (2), 420–445.

Xue, T., Zhu, T., Zheng, Y., Zhang, Q., 2019. Declines in mental health associated with air pollution and temperature variability in China. *Nat. Commun.* 10 (1), 2165.

Zhang, X., Chen, X., Zhang, X., 2018. The impact of exposure to air pollution on cognitive performance. *Proc. Natl. Acad. Sci.* 115 (37), 9193–9197.

Zheng, X., Yang, L., Liu, Y., 2023. The impact of air pollution on outpatient medical service utilization and expenditure in a clean air city. *Soc. Sci. Med.* 338, 116301.